US 20190003003A1

(19) United States
(12) Patent Application Publication
(10) Pub. No.: US 2019/0003003 A1
(43) Pub. Date: Jan. 3, 2019
BRANAGAN et al.

(54) **RETENTION OF MECHANICAL PROPERTIES IN STEEL ALLOYS AFTER PROCESSING AND IN THE PRESENCE OF STRESS CONCENTRATION SITES**

(71) Applicant: **The NanoSteel Company, Inc.**, Providence, RI (US)

(72) Inventors: **Daniel James BRANAGAN**, Idaho Falls, ID (US); **Alla V. SERGUEEVA**, Idaho Falls, ID (US); **Brian E. MEACHAM**, Idaho Falls, ID (US); **Andrew E. FRERICHS**, Idaho Falls, ID (US); **Sheng CHENG**, Idaho Falls, ID (US); **Scott T. LARISH**, Idaho Falls, ID (US); **Grant G. JUSTICE**, Idaho Falls, ID (US); **Andrew T. BALL**, Reno, NV (US); **Jason K. WALLESER**, Idaho Falls, ID (US); **Logan J. TEW**, Idaho Falls, ID (US); **Scott T. ANDERSON**, Idaho Falls, ID (US); **Kurtis R. CLARK**, Idaho Falls, ID (US); **Taylor L. GIDDENS**, Idaho Falls, ID (US)

(73) Assignee: **The NanoSteel Company, Inc.**, Providence, RI (US)

(21) Appl. No.: **16/021,251**

(22) Filed: **Jun. 28, 2018**

Related U.S. Application Data

(60) Provisional application No. 62/527,400, filed on Jun. 30, 2017.

Publication Classification

(51) **Int. Cl.**

C21D 9/46	(2006.01)
C22C 38/58	(2006.01)
C22C 38/42	(2006.01)
C22C 38/34	(2006.01)
C21D 8/02	(2006.01)
C21D 6/00	(2006.01)
B21B 1/22	(2006.01)
B21B 3/00	(2006.01)

(52) **U.S. Cl.**

CPC ***C21D 9/46*** (2013.01); ***C22C 38/58*** (2013.01); ***C22C 38/42*** (2013.01); ***C22C 38/34*** (2013.01); ***C21D 8/0226*** (2013.01); *B21B 2001/225* (2013.01); ***C21D 6/008*** (2013.01); ***C21D 6/005*** (2013.01); ***C21D 6/004*** (2013.01); ***B21B 1/22*** (2013.01); ***B21B 3/00*** (2013.01); ***C21D 8/0205*** (2013.01)

(57) **ABSTRACT**

This invention is related to retention of mechanical properties in high strength steel at reduced thicknesses and which mechanical property performance is also retained at relatively high strain rates. These new steels can offer advantages for a myriad of applications where reduced sheet thickness is desirable. In addition, the alloys herein are those that retain useful mechanical properties after introduction of a geometric discontinuity and an accompanying stress concentration.

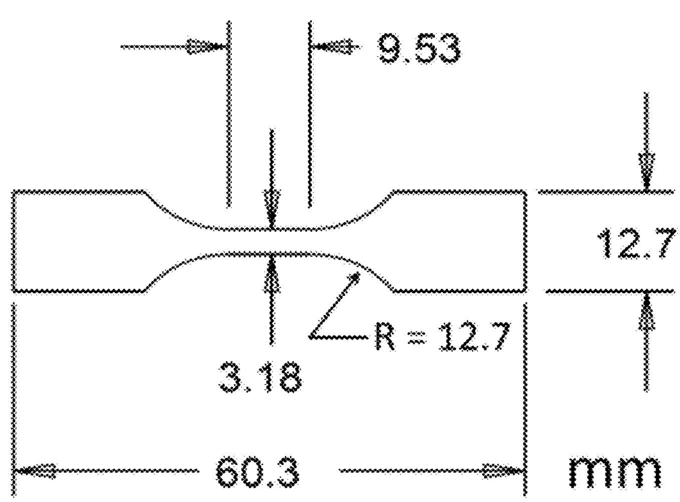

Schematic illustration of the ASTM D 638 Type V tensile specimen geometry; all dimensions are in millimeters.

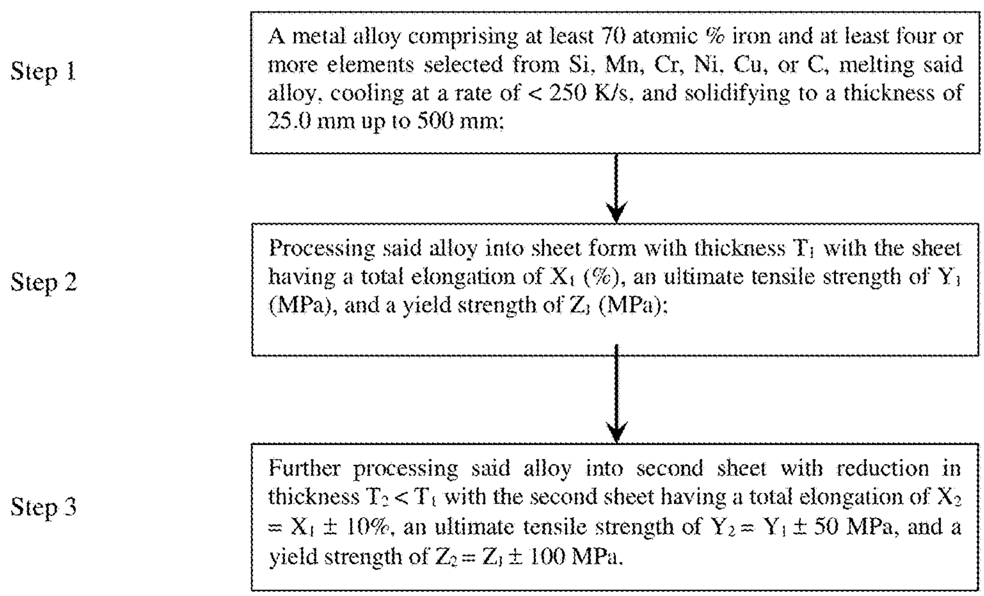

FIG. 1 Summary of the retention of mechanical properties in alloys herein at reduced thicknesses.

Step 1

A metal alloy comprising at least 70 atomic % iron and at least four or more elements selected from Si, Mn, Cr, Ni, Cu, Mo, V, Nb or C, melting said alloy, cooling at a rate of < 250 K/s, and solidifying to a thickness of 25.0 mm up to 500 mm;

↓

Step 2

Processing said alloy into sheet form with thickness T_1 of 1.2 mm to 10.0 mm with the sheet having a total elongation of X_1 (%), an ultimate tensile strength of Y_1 (MPa), and a yield strength of Z_1 (MPa) when tested at strain rate S_1;

↓

Step 3

Deforming the sheet from said alloy at strain rate $S_2 > S_1$ with the sheet having a total elongation of $X_3 = X_1 \pm 7\%$, ultimate tensile strength $Y_3 = Y_1 \pm 200$ MPa, and yield strength $Z_3 = Z_1 \pm 50$ MPa.

FIG. 2 Summary of mechanical property retention in the alloys herein at relatively high strain rates.

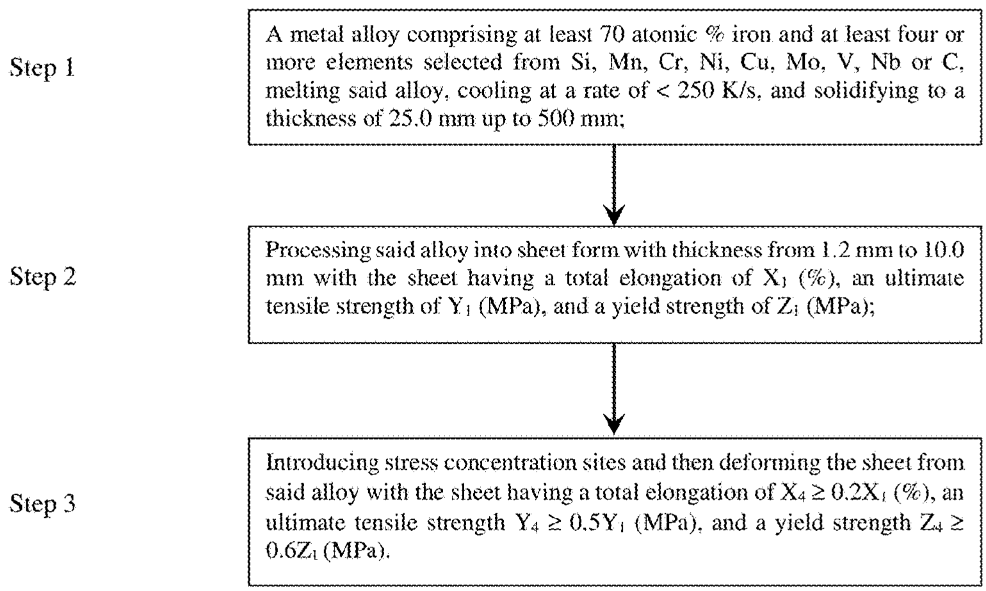

FIG. 3 Summary of retained mechanical properties in the alloys herein with introduced stress concentration sites

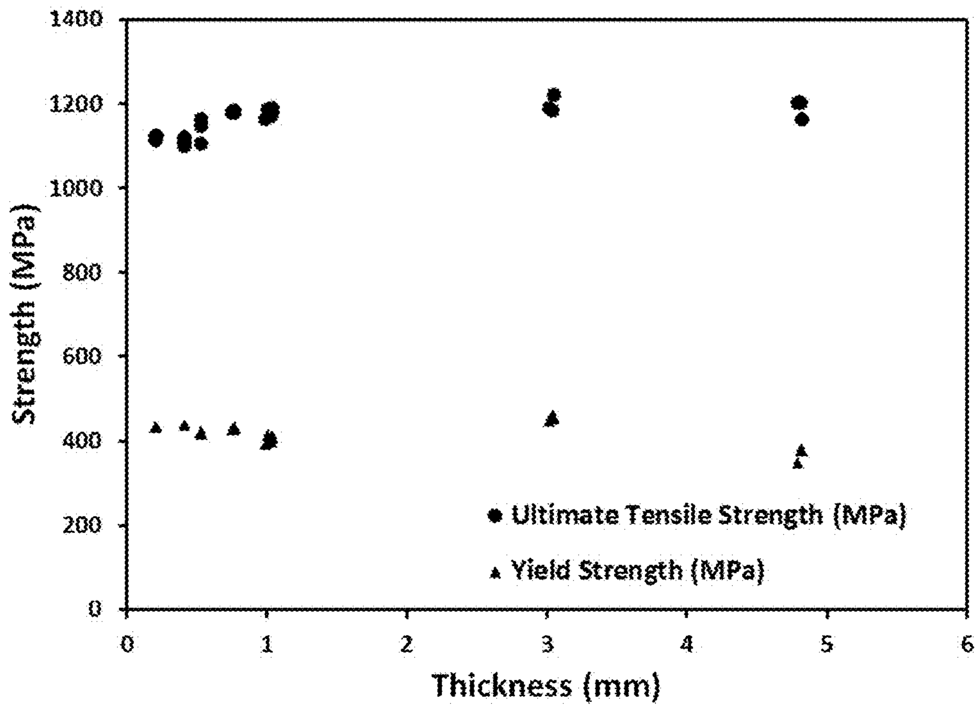

FIG. 4 Yield strength and ultimate tensile strength as a function of the Alloy 2 sheet thickness.

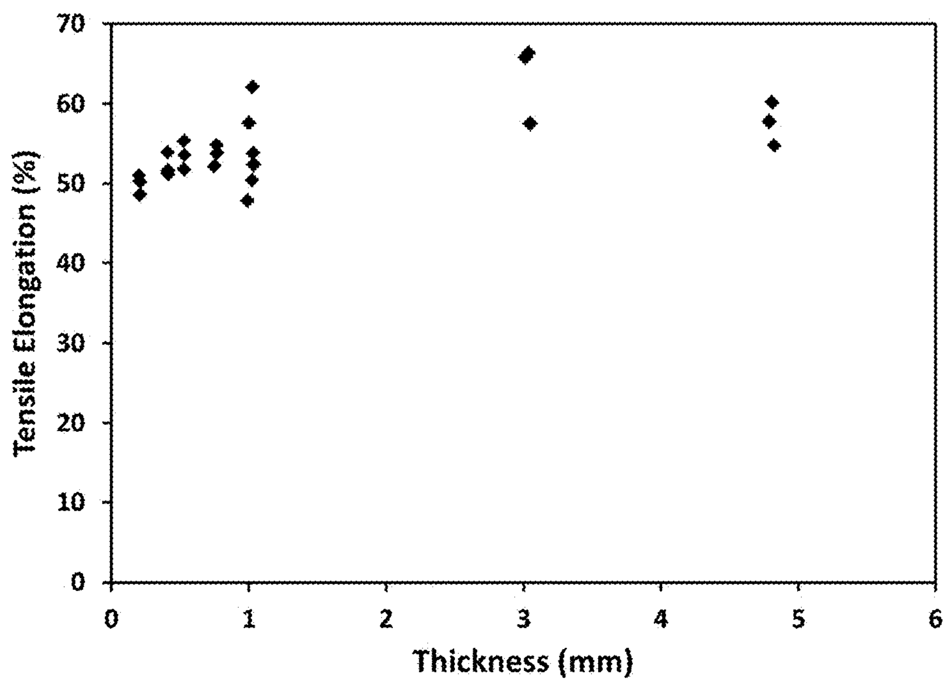

FIG. 5 Tensile elongation as a function of the Alloy 2 sheet thickness.

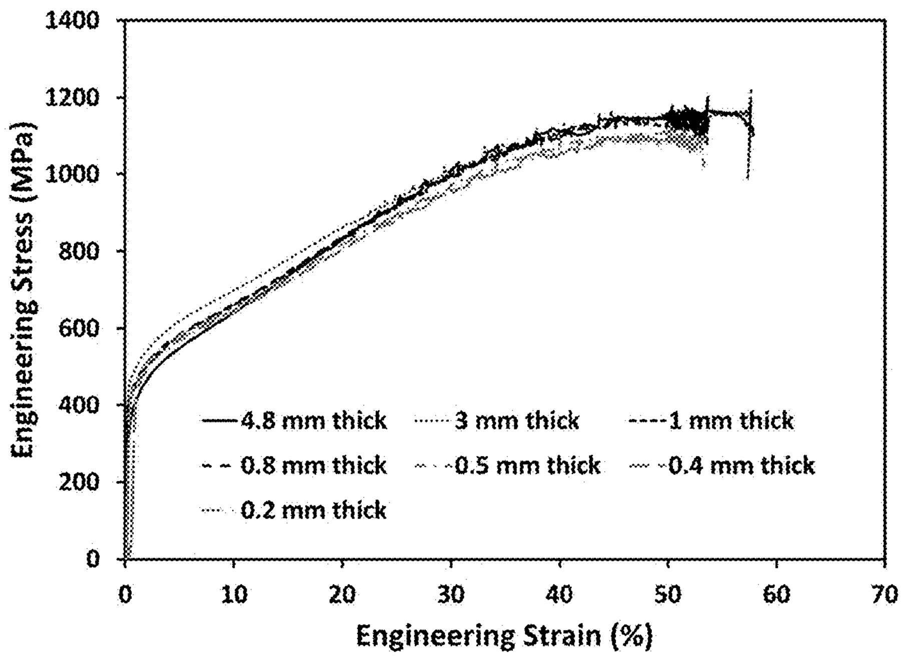

FIG. 6 Comparison of stress - strain curves for Alloy 2 sheet with different thicknesses.

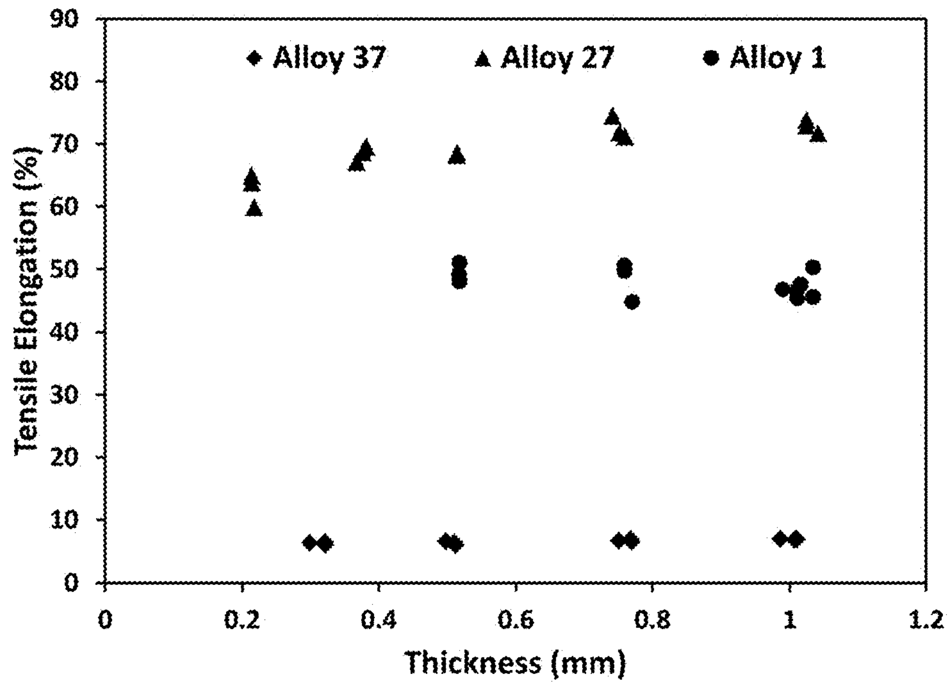

FIG. 7 Effect of sheet thickness on tensile elongation of samples from various alloys.

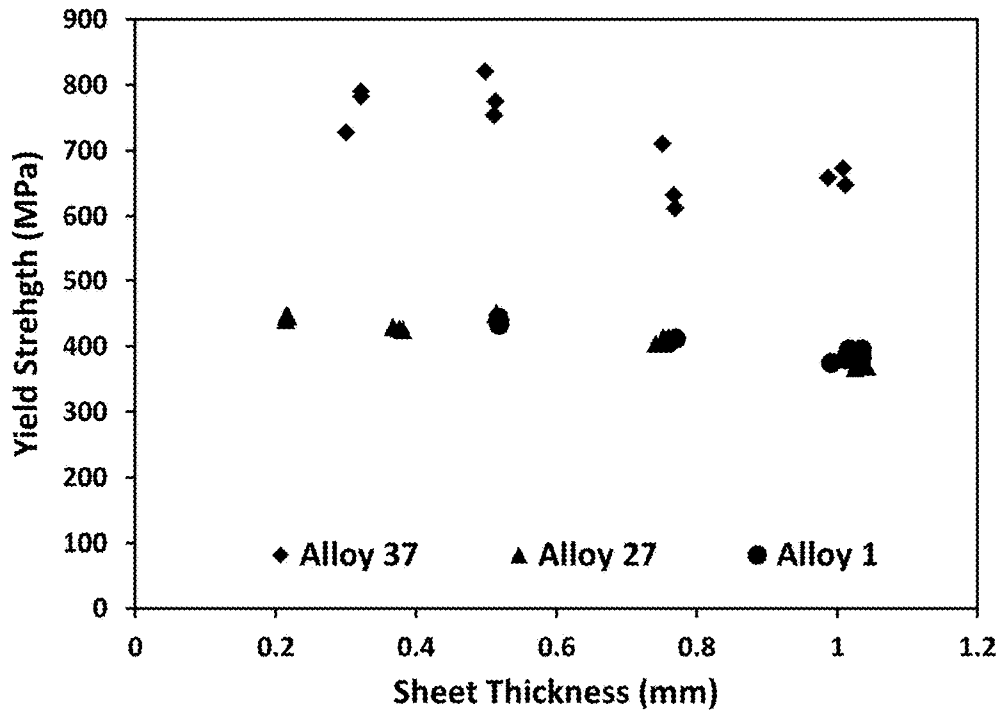

FIG. 8 Effect of sheet thickness on yield strength in samples from various alloys.

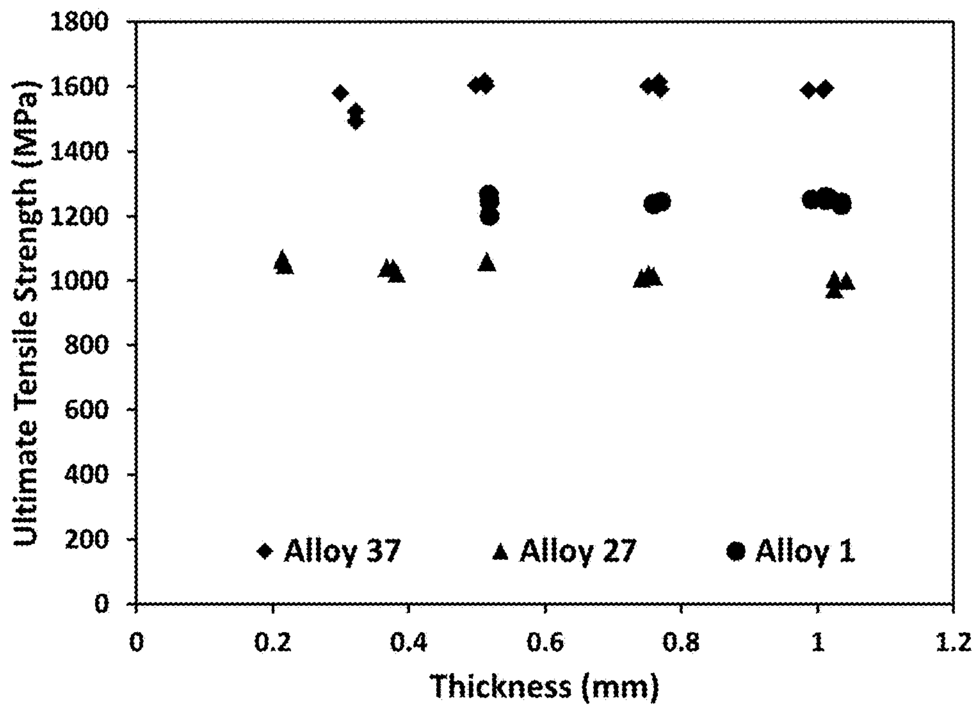

FIG. 9 Effect of sheet thickness on ultimate tensile strength in samples from various alloys.

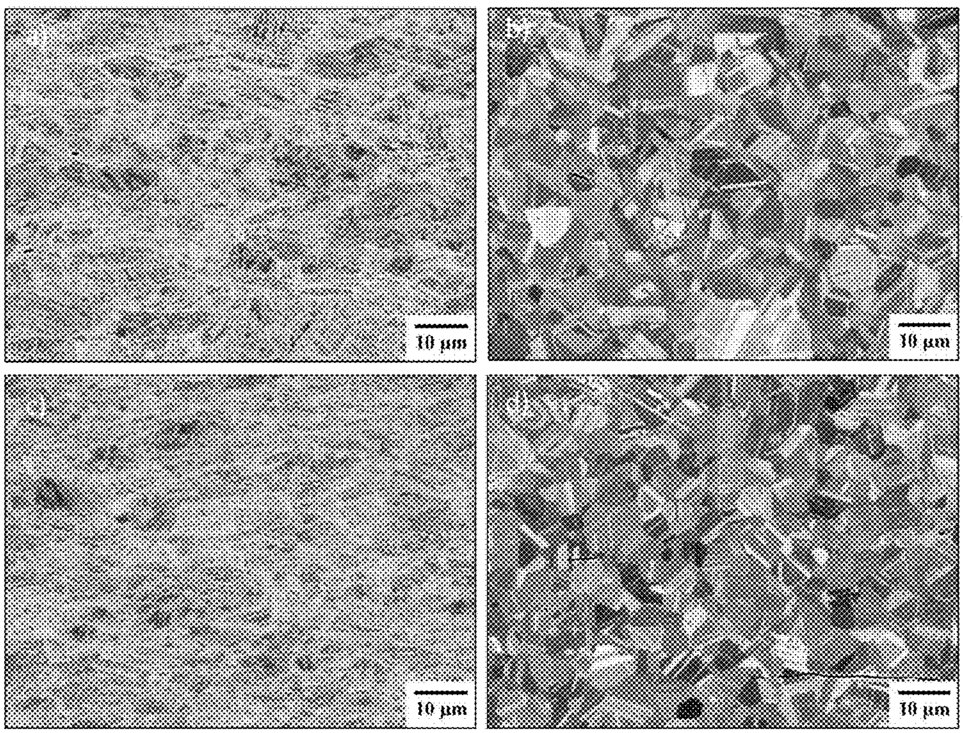

FIG. 10 SEM images of the microstructure in the center of Alloy 1 sheet samples with different thicknesses; a) 0.7 mm thick cold rolled sheet, b) 0.7 mm thick cold rolled and annealed sheet, c) 0.5 mm thick cold rolled sheet, and d) 0.5 mm thick cold rolled and annealed sheet.

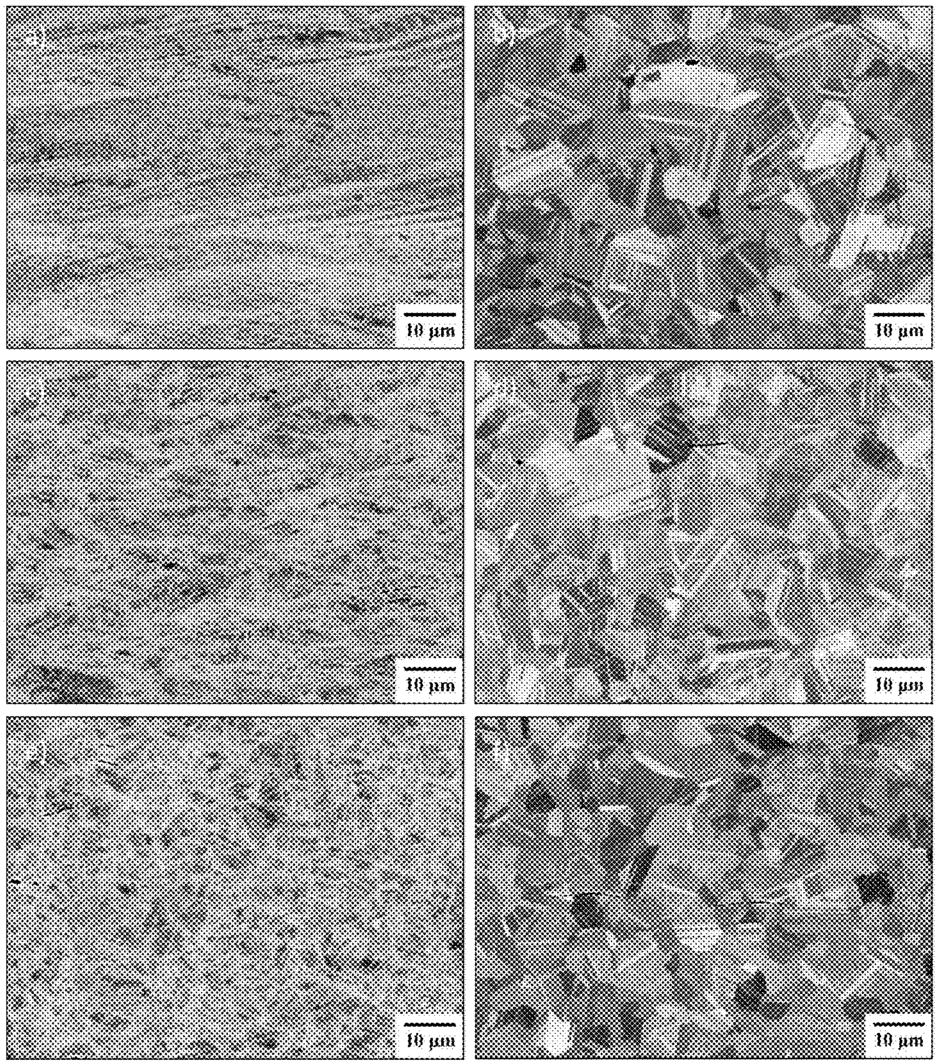

FIG. 11 SEM images of the microstructure in the center of Alloy 2 sheet samples with different thicknesses; a) 1.0 mm thick cold rolled sheet, b) 1.0 mm thick cold rolled and annealed sheet, c) 0.5 mm thick cold rolled sheet, d) 0.5 mm thick cold rolled and annealed sheet, e) 0.2 mm thick cold rolled sheet, and f) 0.2 mm thick cold rolled and annealed sheet.

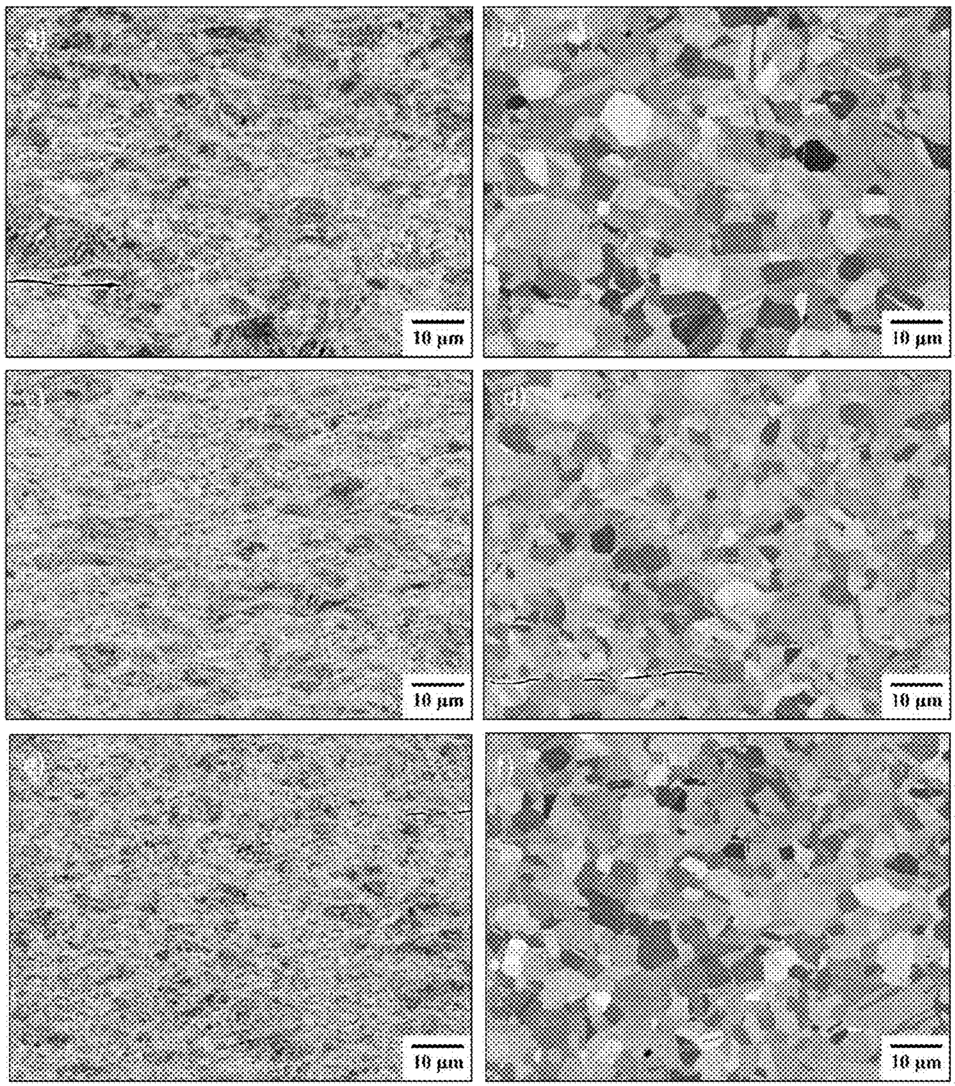

FIG. 12 SEM images of the microstructure in the center of Alloy 27 sheet samples with different thicknesses; a) 0.8 mm thick cold rolled sheet, b) 0.8 mm thick cold rolled and annealed sheet, c) 0.5 mm thick cold rolled sheet, d) 0.5 mm thick cold rolled and annealed sheet, e) 0.4 mm thick cold rolled sheet, and f) 0.4 mm thick cold rolled and annealed sheet.

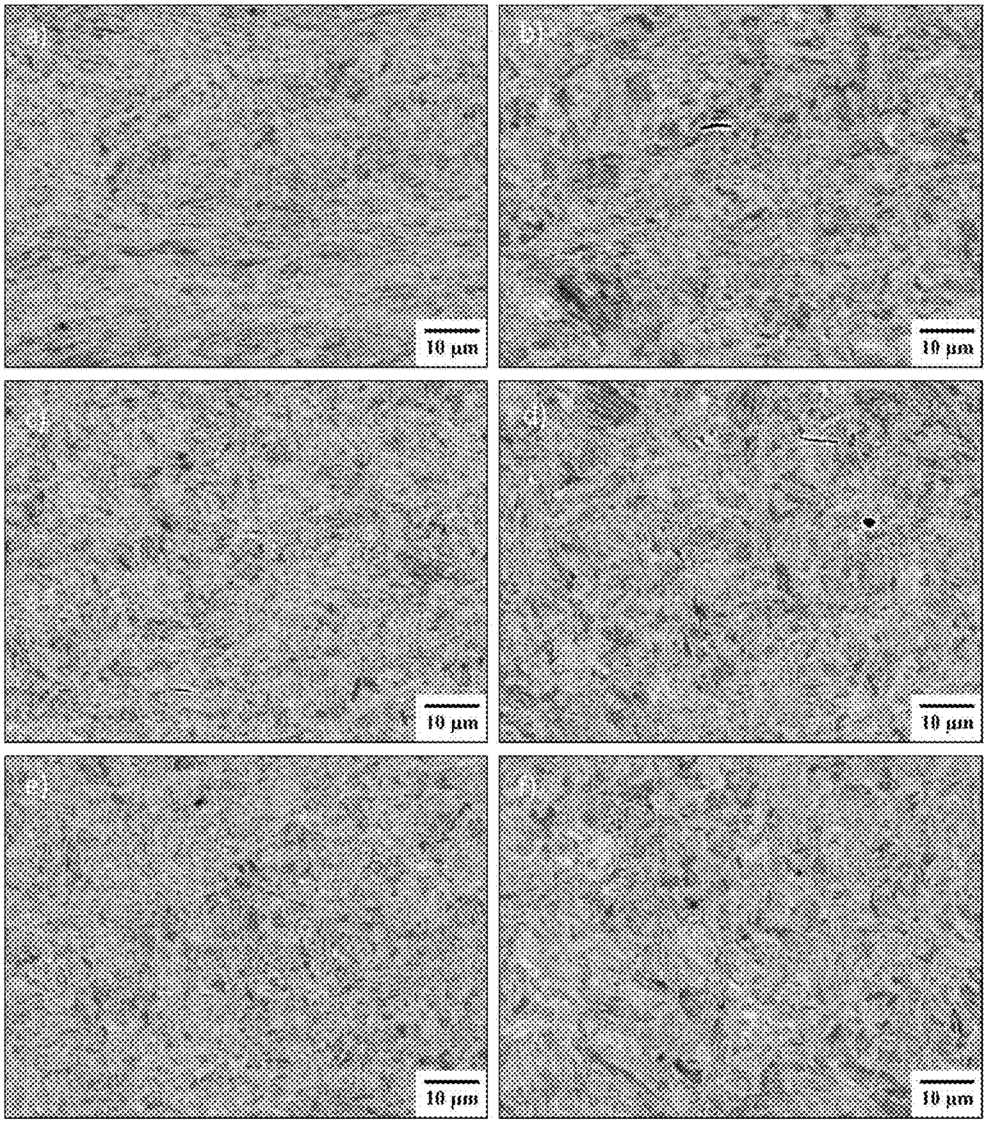

FIG. 13 SEM images of the microstructure in the center of Alloy 37 sheet samples with different thicknesses; a) 1.4 mm thick cold rolled sheet, b) 1.4 mm thick cold rolled and annealed sheet, c) 0.5 mm thick cold rolled sheet, d) 0.5 mm thick cold rolled and annealed sheet, e) 0.3 mm thick cold rolled sheet, and f) 0.3 mm thick cold rolled and annealed sheet.

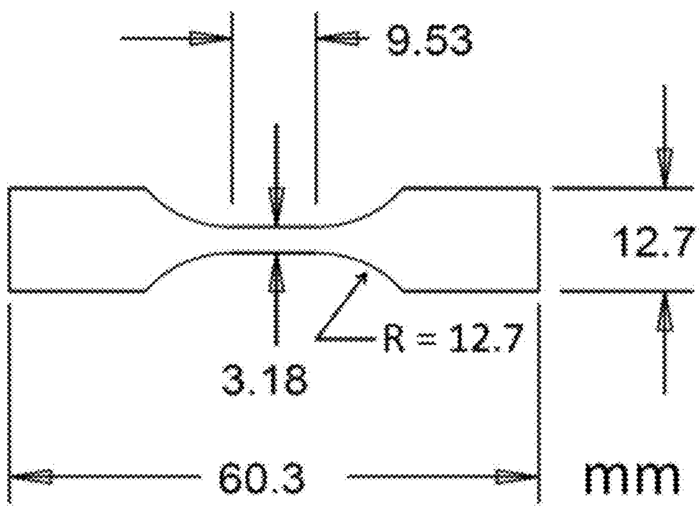

FIG. 14 Schematic illustration of the ASTM D 638 Type V tensile specimen geometry; all dimensions are in millimeters.

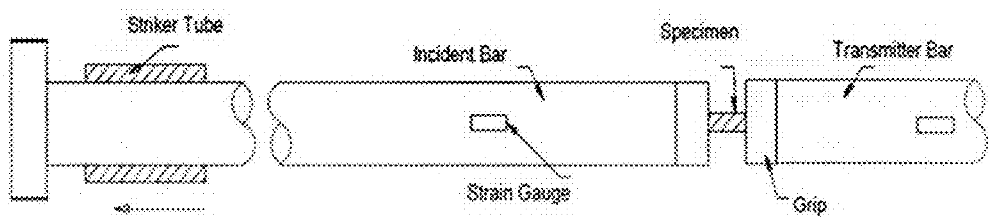

FIG. 15 Schematic diagram of the direct tension split Hopkinson bar (SHB) device.

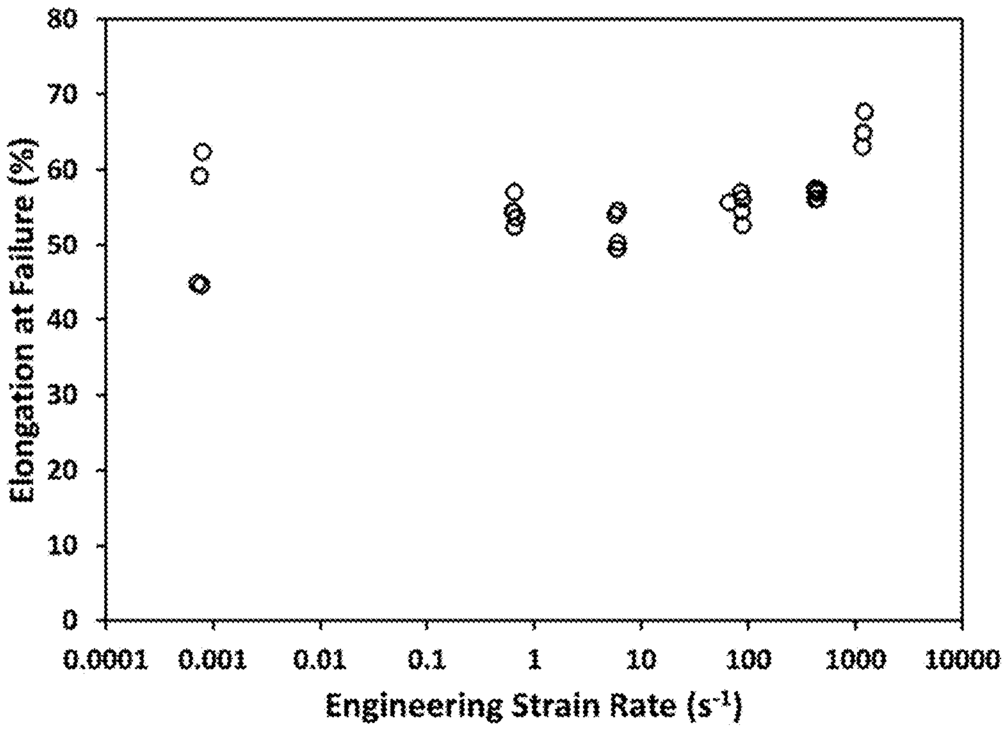

FIG. 16 Effect of strain rate on the tensile elongation at fracture for Alloy 2 sheet.

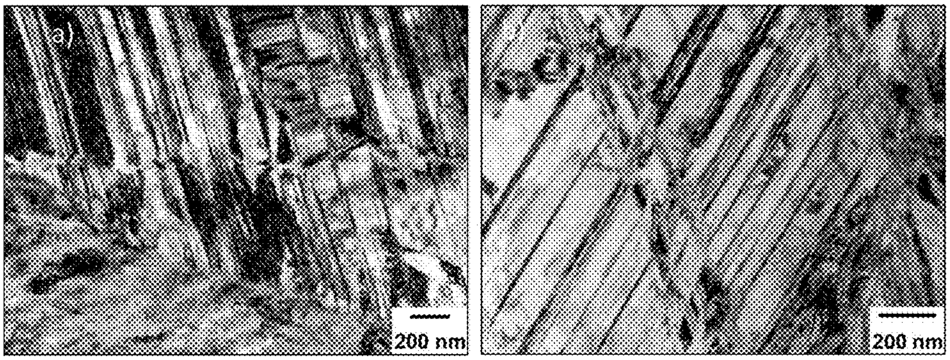

FIG. 17 Bright-field TEM micrographs of the microstructure in gauge section of the sample from Alloy 2 sheet tested at strain rate of 1200 s^{-1}; a) lower magnification image, b) higher magnification image.

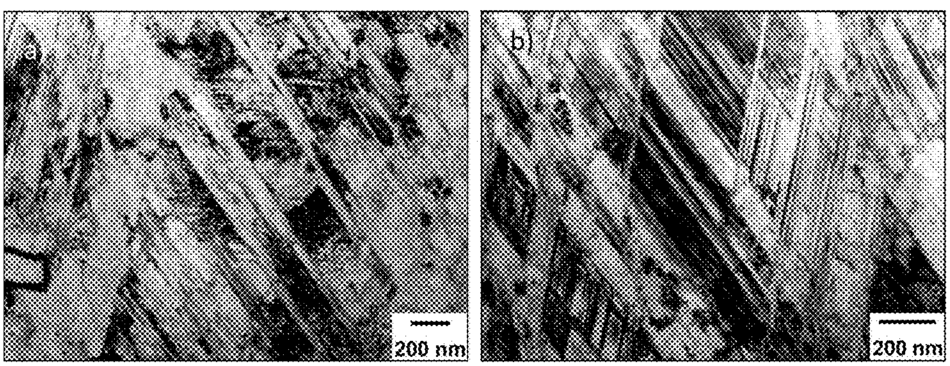

FIG. 18 Bright-field TEM micrographs of the microstructure in gauge section of the sample from Alloy 2 sheet tested at strain rate of 500 s^{-1}; a) lower magnification image, b) higher magnification image.

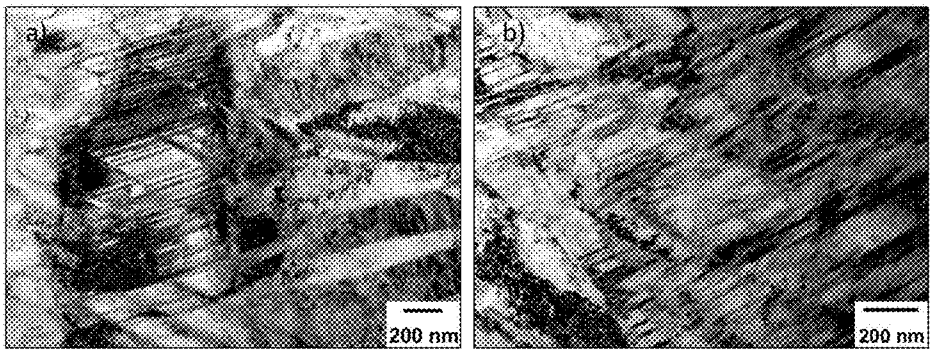

FIG. 19 Bright-field TEM micrographs of the microstructure in gauge section of the sample from Alloy 2 sheet tested at strain rate of 100 s^{-1}; a) lower magnification image, b) higher magnification image.

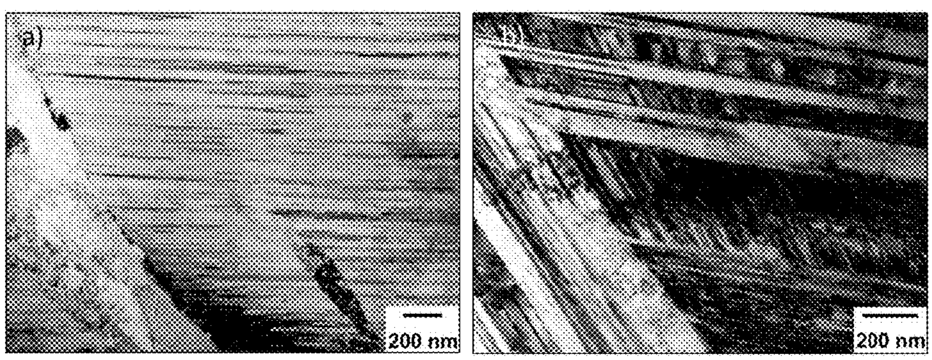

FIG. 20 Bright-field TEM micrographs of the microstructure in gauge section of the sample from Alloy 2 sheet tested at strain rate of 10 s^{-1}; a) lower magnification image, b) higher magnification image.

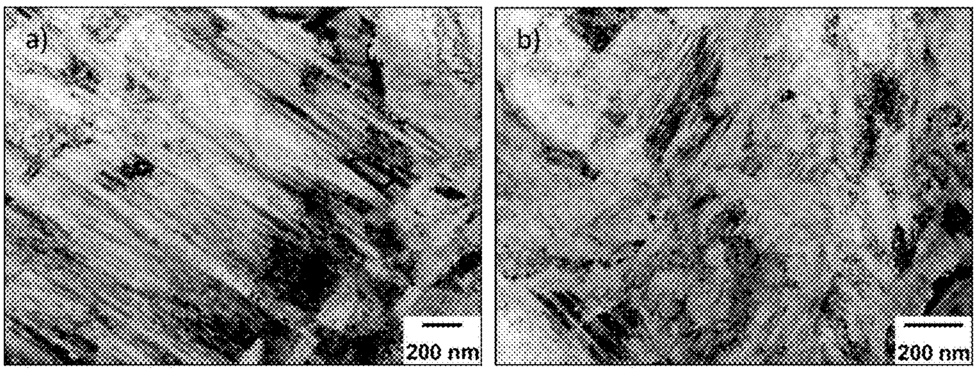

FIG. 21 Bright-field TEM micrographs of the microstructure in gauge section of the sample from Alloy 2 sheet tested at strain rate of 0.7 s^{-1}; a) lower magnification image, b) higher magnification image.

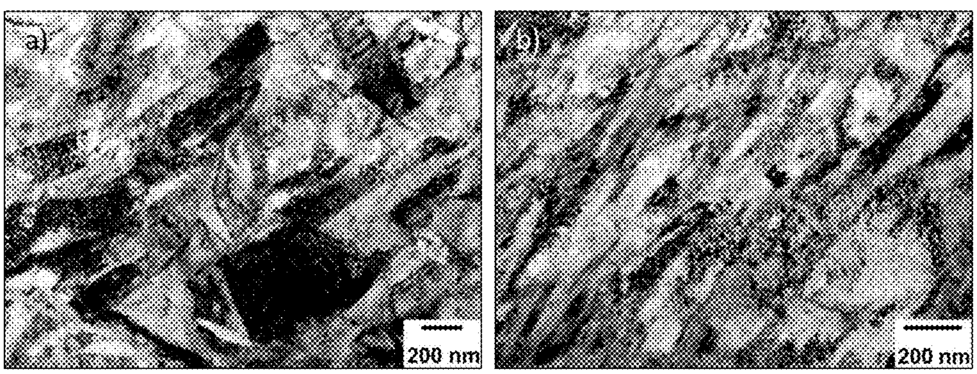

FIG. 22 Bright-field TEM micrographs of the microstructure in gauge section of the sample from Alloy 2 sheet tested at strain rate of 0.0007 s^{-1}; a) lower magnification image, b) higher magnification image.

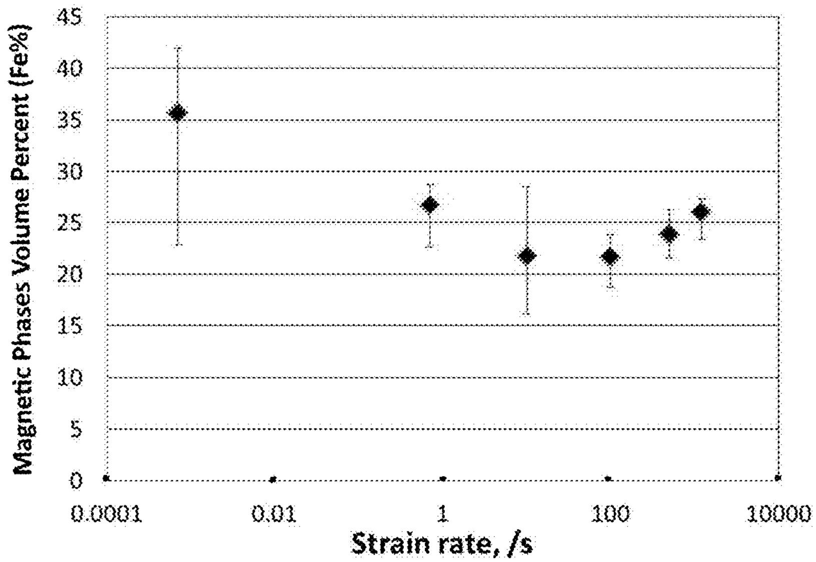

FIG. 23 Feritscope measurements at the gauge section of the samples from Alloy 2 sheet tested at different strain rates.

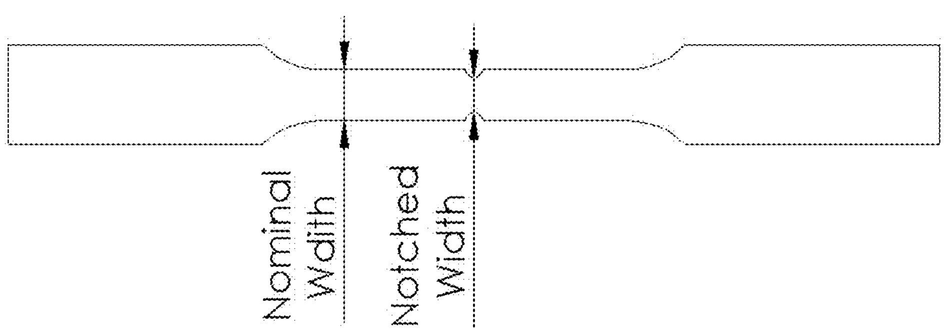

FIG. 24 Schematic illustration of the notched tensile sample.

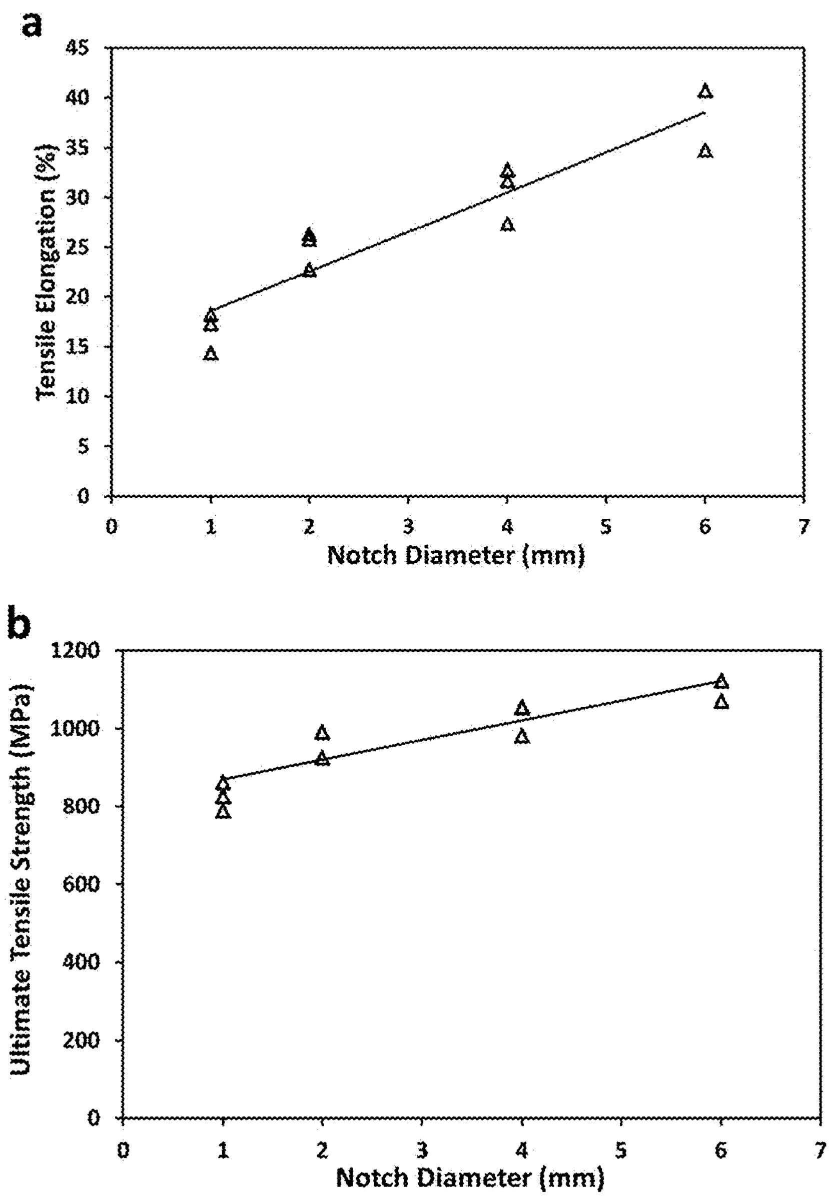

FIG. 25 Notch diameter with a constant depth of 0.5 mm effect; a) on tensile elongation and b) on ultimate tensile strength of the sheet from Alloy 2.

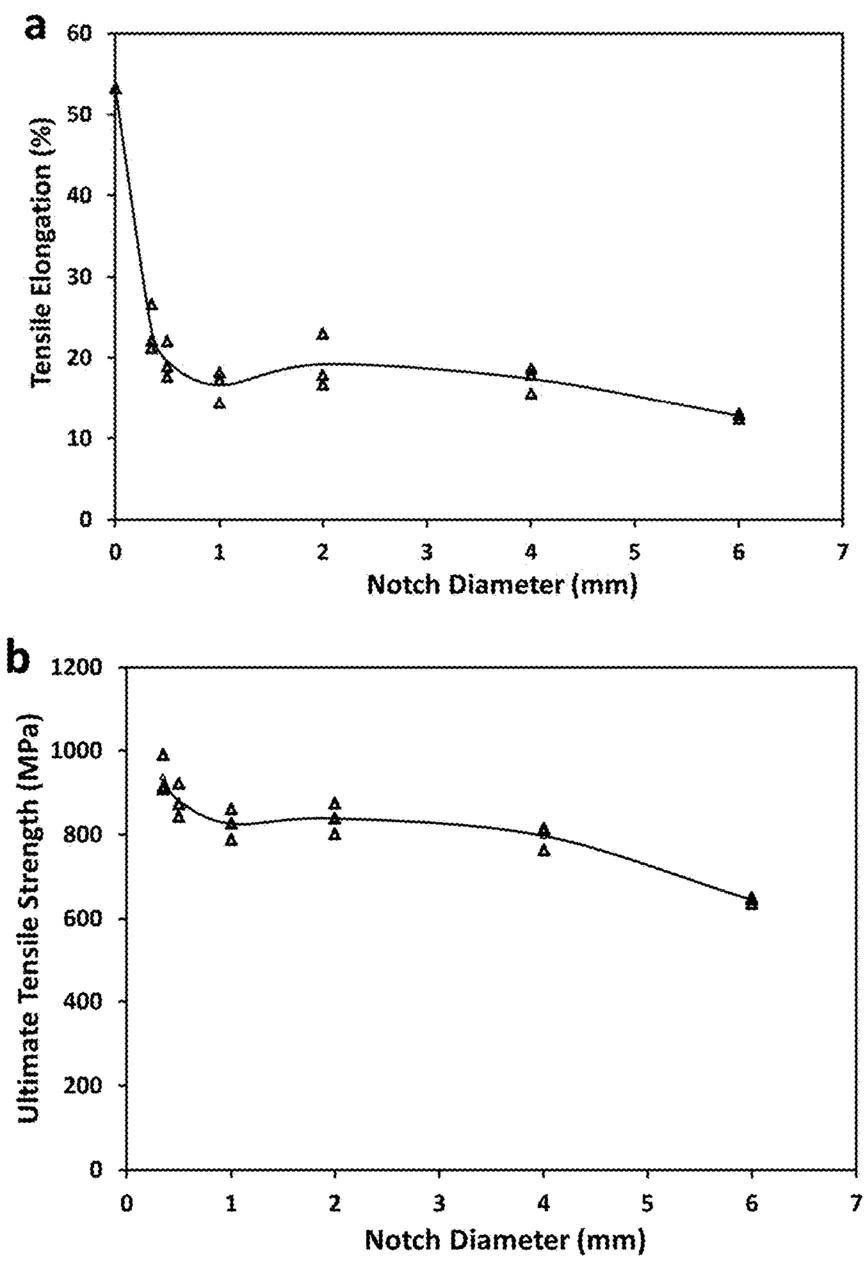

FIG. 26 Half circle notch diameter effect; a) on tensile elongation and b) on ultimate tensile strength of the sheet from Alloy 2.

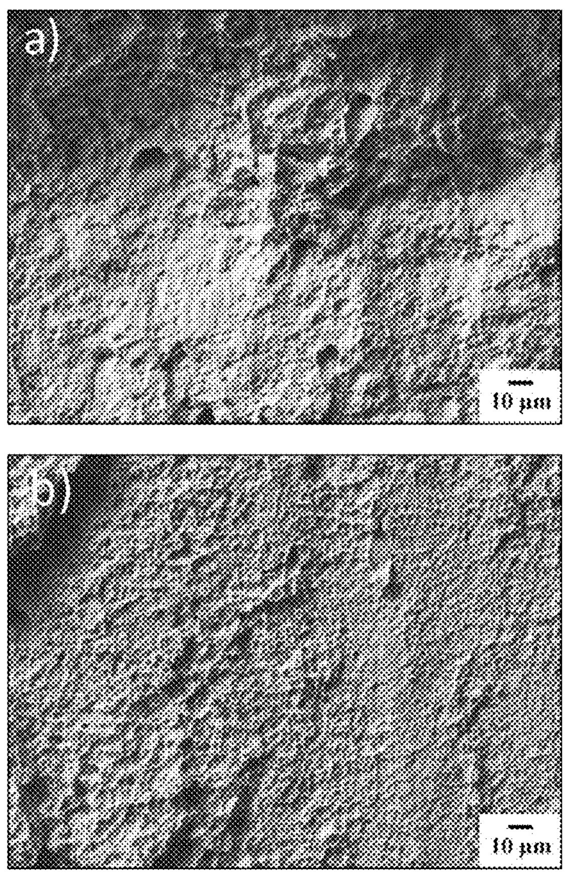

FIG. 27 SEM images of the fracture surface in the Sample 1 from Alloy 2 with a notch of 1 mm in diameter; a) in the center of the fracture cross section, b) near the edge of the fracture cross section.

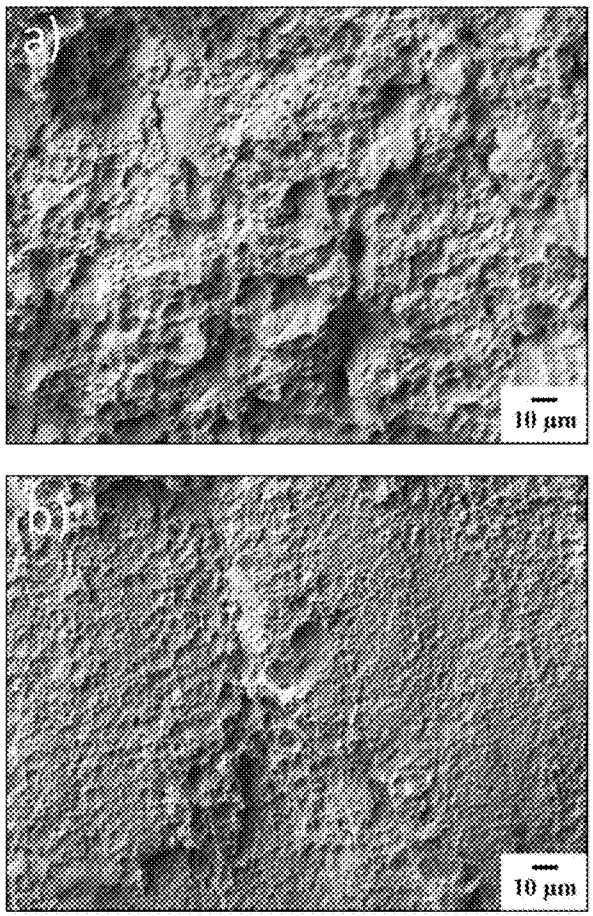

FIG. 28 SEM images of the fracture surface in the Sample 2 from Alloy 2 with a notch of 6 mm in diameter; a) in the center of the fracture cross section, b) near the edge of the fracture cross section.

RETENTION OF MECHANICAL PROPERTIES IN STEEL ALLOYS AFTER PROCESSING AND IN THE PRESENCE OF STRESS CONCENTRATION SITES

FIELD OF INVENTION

[0001] This disclosure is related to retention of mechanical properties in high strength steel at reduced thicknesses and which mechanical property performance is also retained at relatively high strain rates. These new steels can offer advantages for a myriad of applications where reduced sheet thickness is desirable. In addition, the alloys herein are those that retain useful mechanical properties after introduction of a geometric discontinuity and an accompanying stress concentration.

BACKGROUND

[0002] Steel is the engineering material of choice where cost, strength, and ductility are major factors. Accordingly, steel continues to be used in a myriad of applications in our daily lives, including in the construction of buildings, appliances, and automobiles. A large variety of steel alloys exist to achieve this range of needs, with targeted property ranges used for these wide ranging applications. Designations are provided for ranges of steel, which fit three distinct classes based upon measured properties, in particular maximum tensile strain and tensile stress prior to failure. These three classes are: Low Strength Steels (LSS), High Strength Steels (HSS), and Advanced High Strength Steels (AHSS). Advanced High Strength Steels (AHSS) are of primary interest for advanced engineering applications, and are classified by tensile strengths greater than 700 MPa and include such types as martensitic steels (MS), dual phase (DP) steels, transformation induced plasticity (TRIP) steels, and complex phase (CP) steels. As the strength level increases the trend in maximum tensile elongation (ductility) of the steel is negative, with decreasing elongation at high tensile strengths. For example, tensile elongation of LSS, HSS and AHSS ranges from 25% to 55%, 10% to 45%, and 4% to 30%, respectively.

[0003] An area where steel provides particular engineering advantages is in automobiles, with many different types of steels utilized throughout the car in various locations. Current consumer desires and governmental regulations are pushing automobile manufacturers to design vehicles that attain ever greater fuel efficiency. Automobile designers have identified weight reduction, particularly in the body-in-white structure, to have the greatest potential impact on improving fuel efficiency. The process of reducing automobile weight, known as lightweighting, can be accomplished through reducing the thickness of the body-in-white structure and increasing the geometric complexity of the various parts using high strength, high formability materials. Accordingly, increasingly high strength steels are desired throughout the automobile assembly in order to enable the thickness reduction and weight savings.

[0004] Safety must be kept constant or improved during the lightweighting process as well. Automobile highway speed limits are regularly increasing, and consumers expect safety performance to be a major part of automobile design. The body-in-white structure of an automobile is designed to provide a rigid structure that will protect the passenger while traveling at speed and in the case of a collision. During an automobile collision, dynamic loading, rapid deformation, and energy dissipation occurs throughout the automobile and body-in-white structure in particular. The time frame over which this occurs can be 100 ms. High strain rates are observed throughout the body-in-white structure during this time, and materials need to be able to withstand complex loads across a range of strain rates. For instance, a low speed collision that occurs in a parking lot would result in a lower strain rate for body-in-white than would a collision at highway speeds. The mechanical properties of materials for the body-in-white structure are measured by many means, including uniaxial tensile testing, across this range of strain rates such that their response during a collision can be predicted and design considerations taken into account. High strain rates can result in a change in mechanical properties, limiting the maximum lightweighting that automobile designers are able to achieve by requiring additional thickness to maintain safety under high strain rate conditions.

[0005] As advances in engineering and technology occur, there is an increasing drive to the small scale. Consumers, and by extension engineers/designers, are regularly searching for products that are size efficient. Consumers seek out products that accomplish the needed task while occupying the smallest volume possible. A good example of this phenomenon can be found in the electronics industry, where cell phones, tablets, and other devices are regularly reduced in size with consecutive design iterations. With the drive of products to smaller and smaller sizes, the demands on engineering materials that the products are made from increase dramatically. As the overall size of a part decreases, defects that are inherent in everyday manufacturing processes can result in significant reductions in material properties. High strength materials are particularly impacted by the reduction of part size to the small or very small due to the complex and often specialized processing required to achieve those properties.

[0006] Martensitic steels, for example, provide excellent strength yet require a quench as a final processing step to create the necessary microstructure. Quenching is difficult to control at a small scale and may potentially cause unacceptable distortion in small parts. Final processing may not be performed on the final part geometry but rather on sheet or foils in some applications. For thermally sensitive materials such as martensitic steels, thermal exposure during cutting to produce the final part may detrimentally alter the microstructure and compromise properties. Geometry effects also play a greater role in mechanical properties of ductile materials at the small scale, with the effects of stress concentrators, grain size, and thickness adversely changing the material's mechanical response to stress. Due to these facts, expensive engineering materials are often required for uses on small scale that are either thermally insensitive or have simple processing such as low alloyed or pure materials. Engineers would prefer to not use exotic materials for these applications; however everyday engineering materials are often unavailable for use at reduced thicknesses resulting in the slow adoption of smaller devices due to prohibitive cost and processing requirements.

SUMMARY

[0007] In one embodiment, the present invention is directed at a method to retain mechanical properties in a metallic sheet alloy at reduced thickness comprising supplying a metal alloy comprising at least 70 atomic % iron and at least four or more elements selected from Si, Mn, Cr, Ni, Cu, or C, melting said alloy, cooling at a rate of <250 K/s, and solidifying to a thickness of 25.0 mm up to 500 mm. This is followed by processing the alloy into sheet form with thickness T_1 with the sheet having a total elongation of X_1 (%), an ultimate tensile strength of Y_1 (MPa), and a yield strength of Z_1 (MPa). This is then followed by further processing the alloy into a second sheet with reduction in thickness $T_2<T_1$ with the second sheet having a total elongation of $X_2=X_1\pm10\%$, an ultimate tensile strength of $Y_2=Y_1\pm50$ MPa, and a yield strength of $Z_2=Z_1\pm100$ MPa.

[0008] In another embodiment the present invention relates to a method to retain mechanical properties in a metallic sheet alloy at relatively high strain rates comprising supplying a metal alloy comprising at least 70 atomic % iron and at least four or more elements selected from Si, Mn, Cr, Ni, Cu, or C and melting said alloy and cooling at a rate of <250 K/s and solidifying to a thickness of 25.0 mm up to 500 mm. This is then followed by processing the alloy into sheet form with thickness from 1.2 mm to 10.0 mm with the sheet having a total elongation of X_1 (%), an ultimate tensile strength of Y_1 (MPa), and a yield strength of Z_1 (MPa) when tested at a strain rate S_1. This is then followed by deforming the sheet from the alloy at a strain rate $S_2>S_1$ with the sheet having a total elongation of $X_3=X_1\pm7\%$, ultimate tensile strength $Y_3=Y_1\pm200$ MPa, and yield strength $Z_3=Z_1\pm50$ MPa.

[0009] In yet another embodiment the present invention is directed at A method to retain mechanical properties in a metallic sheet alloy comprising supplying a metal alloy comprising at least 70 atomic % iron and at least four or more elements selected from Si, Mn, Cr, Ni, Cu, or C and melting said alloy and cooling at a rate of <250 K/s and solidifying to a thickness of 25.0 mm up to 500 mm. This is then followed by processing the alloy into sheet form with thickness from 1.2 mm to 10.0 mm with the sheet having a total elongation of X_1 (%), an ultimate tensile strength of Y_1 (MPa), and a yield strength of Z_1 (MPa). Then, one may introduce stress concentration sites and then deform the sheet from the alloy with the sheet having a total elongation of $X_4\le0.2X_1$ (%), an ultimate tensile strength $Y_4\le0.5Y_1$ (MPa), and a yield strength $Z_4\ge0.6Z_1$ (MPa).

BRIEF DESCRIPTION OF THE DRAWINGS

[0010] The detailed description below may be better understood with reference to the accompanying FIG.s which are provided for illustrative purposes and are not to be considered as limiting any aspect of this invention.

[0011] FIG. **1** Summary of novel ductility achievement in alloys herein at reduced length scales.

[0012] FIG. **2** Summary of novel ductility achievement in the alloys herein at high strain rates.

[0013] FIG. **3** Summary of maintained ductility in the alloys herein with introduced stress concentration sites such as edge notches.

[0014] FIG. **4** Yield strength and ultimate tensile strength as a function of Alloy 2 sheet thickness.

[0015] FIG. **5** Tensile elongation as a function of Alloy 2 sheet thickness.

[0016] FIG. **6** Comparison of stress-strain curves for Alloy 2 sheet with different thicknesses.

[0017] FIG. **7** Effect of sheet thickness on tensile elongation of samples from various alloys.

[0018] FIG. **8** Effect of sheet thickness on yield strength in samples from various alloys.

[0019] FIG. **9** Effect of sheet thickness on ultimate tensile strength in samples from various alloys.

[0020] FIG. **10** SEM images of the microstructure in the center of Alloy 1 sheet samples with various thicknesses; a) 0.7 mm thick cold rolled sheet, b) 0.7 mm thick cold rolled and annealed sheet, c) 0.5 mm thick cold rolled sheet, and d) 0.5 mm thick cold rolled and annealed sheet.

[0021] FIG. **11** SEM images of the microstructure in the center of Alloy 2 sheet samples with various thicknesses; a) 1.0 mm thick cold rolled sheet, b) 1.0 mm thick cold rolled and annealed sheet, c) 0.5 mm thick cold rolled sheet, d) 0.5 mm thick cold rolled and annealed sheet, e) 0.2 mm thick cold rolled sheet, and f) 0.2 mm thick cold rolled and annealed sheet.

[0022] FIG. **12** SEM images of the microstructure in the center of Alloy 27 sheet samples with various thicknesses; a) 0.8 mm thick cold rolled sheet, b) 0.8 mm thick cold rolled and annealed sheet, c) 0.5 mm thick cold rolled sheet, d) 0.5 mm thick cold rolled and annealed sheet, e) 0.4 mm thick cold rolled sheet, and f) 0.4 mm thick cold rolled and annealed sheet.

[0023] FIG. **13** SEM images of the microstructure in the center of Alloy 37 sheet samples with various thicknesses; a) 1.4 mm thick cold rolled sheet, b) 1.4 mm thick cold rolled and annealed sheet, c) 0.5 mm thick cold rolled sheet, d) 0.5 mm thick cold rolled and annealed sheet, e) 0.3 mm thick cold rolled sheet, and f) 0.3 mm thick cold rolled and annealed sheet.

[0024] FIG. **14** Schematic illustration of the ASTM D 638 Type V tensile specimen geometry; all dimensions are in millimeters.

[0025] FIG. **15** Schematic diagram of the direct tension split Hopkinson bar (SHB) device.

[0026] FIG. **16** Effect of strain rate on the tensile elongation at fracture for Alloy 2 sheet.

[0027] FIG. **17** Bright-field TEM micrographs of microstructure in gauge section of the sample from Alloy 2 sheet tested at strain rate of 1200 s^{-1}; a) lower magnification image, b) higher magnification image.

[0028] FIG. **18** Bright-field TEM micrographs of microstructure in gauge section of the sample from Alloy 2 sheet tested at strain rate of 500 s^{-1}; a) lower magnification image, b) higher magnification image.

[0029] FIG. **19** Bright-field TEM micrographs of microstructure in gauge section of the sample from Alloy 2 sheet tested at strain rate of 100 s^{-1}; a) lower magnification image, b) higher magnification image.

[0030] FIG. **20** Bright-field TEM micrographs of microstructure in gauge section of the sample from Alloy 2 sheet tested at strain rate of 10 s^{-1}; a) lower magnification image, b) higher magnification image.

[0031] FIG. **21** Bright-field TEM micrographs of microstructure in gauge section of the sample from Alloy 2 sheet tested strain rate of 0.7 s^{-1}; a) lower magnification image, b) higher magnification image.

[0032] FIG. **22** Bright-field TEM micrographs of microstructure in gauge section of the sample from Alloy 2 sheet tested at strain rate of 0.0007 s^{-1}; a) lower magnification image, b) higher magnification image.

[0033] FIG. **23** Feritscope measurements at the gauge section of the samples from Alloy 2 sheet tested at different strain rates.

[0034] FIG. **24** Schematic illustration of the notched tensile sample.

[0035] FIG. **25** Notch diameter with a constant depth of 0.5 mm effect; a) on tensile elongation and b) on ultimate tensile strength of the sheet from Alloy 2.

[0036] FIG. **26** Half circle notch diameter effect; a) on tensile elongation and b) on ultimate tensile strength of the sheet from Alloy 2.

[0037] FIG. **27** SEM images of the fracture surface in the Sample 1 from Alloy 2 with a notch of 1 mm in diameter; a) in the center of the fracture cross section, b) near the edge of the fracture cross section.

[0038] FIG. **28** SEM images of the fracture surface in the Sample 2 from Alloy 2 with a notch of 6 mm in diameter; a) in the center of the fracture cross section, b) near the edge of the fracture cross section.

DETAILED DESCRIPTION OF PREFERRED EMBODIMENTS

[0039] The retention of mechanical properties in the alloys herein at reduced thickness and relatively high strain rates is illustrated in FIG. **1** and FIG. **2**. FIG. **1** represents a summary on mechanical property retention in the alloys herein when reduced in thickness. In Step 1 in FIG. **1**, the starting condition is to supply a metal alloy. This metal alloy will preferably comprise at least 70 atomic % iron and at least four or more elements selected from Si, Mn, Cr, Ni, Cu, or C. The alloy chemistry is melted, cooled at a rate of <250 K/s, and solidified to a thickness of 25.0 mm and up to and including 500 mm. The casting process can be done in a wide variety of processes including ingot casting, bloom casting, continuous casting, thin slab casting, thick slab casting, thin strip casting, belt casting etc. Preferred methods would be continuous casting in sheet form by thin slab casting, thick slab casting, and thin strip casting. Preferred alloys exhibit a fraction of austenite (y-Fe) at least 10 volume percent up to 100 volume percent and all increments in between. The alloy is then processed into sheet form with a thickness T_1 that is in the range of 1.2 mm to 10.0 mm, and therefore includes thicknesses of 1.2 mm, 1.3 mm. 1.4 mm 1.5 mm. 1.6 mm, 1.7 mm, 1.8 mm, 1.9 mm, 2.0 mm, 2.1 mm, 2.2 mm, 2.3 mm, 2.4 mm, 2.5 mm, 2.6 mm, 2.7 mm, 2.8 mm, 2.9 mm, 3.0 mm, 3.1 mm, 3.2 mm, 3.3 mm, 3.4 mm, 3.5 mm, 3.6 mm, 3.7 mm, 3.8 mm, 3.9 mm, 4.0 mm, 4.1 mm, 4.2 mm, 4.3 mm, 4.4 mm, 4.5 mm, 4.6 mm, 4.7 mm, 4.8 mm, 4.9 mm and 5.0 mm, 5.1 mm, 5.2 mm, 5.3 mm. 5.4 mm. 5.5 mm, 5.6 mm, 5.7 mm, 5.8 mm, 5.9 mm, 6.0 mm, 6.1 mm, 6.2 mm, 6.3 mm, 6.4 mm, 6.5 mm, 6.6 mm, 6.7 mm, 6.8 mm, 6.9 mm, 7.0 mm, 7.1 mm, 7.2 mm, 7.3 mm, 7.4 mm, 7.5 mm, 7.6 mm, 7.7 mm, 7.8 mm, 7.9 mm, 8.0 mm, 8.1 mm, 8.2 mm, 8.3 mm, 8.4 mm, 8.5 mm, 8.6 mm, 8.7 mm, 8.8 mm, 8.9 mm, 9.0 mm, 9.1 mm, 9.2 mm, 9.3 mm, 9.4 mm, 9.5 mm, 9.6 mm, 9.7 mm, 9.8 mm, 9.9 mm and 10.0 mm.

[0040] The steps to produce this sheet at thickness T_1 from the cast product can vary depending on specific manufacturing routes and specific targeted goals. As an example, consider thick slab casting as one process route to get to sheet of this targeted thickness. The alloy would be cast going through a water cooled mold typically in a thickness range of 150 to 300 mm in thickness. The cast ingot after cooling would then be preferably prepared for hot rolling which may involve some surface treatment to remove surface defects including oxides. The ingot would then go through a roughing mill hot roller which may involve several passes resulting in a transfer bar slab typically from 15 to 100 mm in thickness. This transfer bar would then go through successive/tandem hot rolling finishing stands to produce hot band coils which have a thickness T_1 in the above referenced range from 1.2 mm to 10.0 mm.

[0041] Another example would be to preferably process the cast material through a thin slab casting process. In this case, after casting typically forms 35 to 150 mm in thickness by going through a water cooled mold, the newly formed slab goes directly to hot rolling without cooling down with auxiliary tunnel furnace or induction heating applied to bring the slab directly up to targeted temperature. The slab is then hot rolled directly in multi-stand finishing mills which are preferably from 1 to 7 in number. After hot rolling, the strip is rolled into hot band coils with thickness T_1 in the above referenced range of 1.2 mm to 10.0 mm in thickness. Note that bloom casting would be similar to the examples above but higher thickness might be cast typically from 200 to 500 mm thick and initial breaker steps would be needed to reduce initial cast thickness to allow it to go through a hot rolling roughing mill. Strip casting would be similar but lower thickness might be cast of T_1 having a value of 1.2 mm to 10.0 mm in thickness with preferably only one hot rolling stand directly after casting.

[0042] Accordingly, the specific process in going from the slab material in Step 1 to a preferred thickness T_1 of 1.2 mm to 10 mm and then in Step 2 to a preferred thickness in the range of 0.2 mm to less than 1.2 mm may include hot rolling, cold rolling, and/or cold rolling followed by annealing. Accordingly, in Step 2, the alloy thickness may preferably be 0.2 mm, 0.3 mm, 0.4 mm. 0.5 mm. 0.6 mm. 0.7 mm. 0.8 mm. 0.9 mm, 1.0 mm 1.1 mm up to by not including 1.2 mm. Hot rolling is generally used to provide a preferred thickness from 1.2 mm to 10.0 mm and is typically done in roughing mills, finishing mills, and/or Steckel mills. Cold rolling is preferred in Steps 1 and/or Step 2 and is generally done using tandem mills, Z-mills, and/or reversing mills. The cold rolled material depending on property targets may be annealed to restore the ductility lost from the cold rolling process either partially or with restoration of ductility. Typically as cold rolling proceeds and higher amounts of gauge reduction occurs, ductility is reduced and cold rolling will continue until or just before cracking is observed. Restoration of the tensile ductility of the cold rolled sheet generally occurs with heat treatments at 700° C. and above. Once the sheet is formed with thickness T_1 specified in Step 2, the sheet will then exhibit a total elongation of X_1 (%), an ultimate tensile strength of Y_1 (MPa), and a yield strength of Z_1 (MPa). Preferred properties for alloys herein in Step 2 would be tensile elongation from 12 to 80%, ultimate tensile strength values from 700 to 2100 MPa, and yield strength is in a range from 250 to 1500 MPa.

[0043] In Step 3, the alloy is preferably cold rolled and annealed in similar manner as in Step 2 to thickness $T_2<T_1$. In Step 3, comparing said alloy in Step 1 and after Step 2, the total elongation is maintained at the level where the total elongation $X_2=X_1\pm10\%$, $Y_2=Y_1\pm50$ MPa, and $Z_2=Z_1\pm100$ MPa. The thickness of the alloy in Step 3 is identified as T_2 and is less than the thickness T_1 in Step 2. The preferred properties of the alloy in Step 3 are as follows: X_2=2 to 90%; Y_2=650 MPa to 2150 MPa and Z_2=150 MPa to 1600 MPa.

[0044] FIG. **2** shows a summary on ductility retention of the present disclosure in the alloys herein at relatively high strain rates, that is where the alloys experience a strain rate of S_2 of >0.007 to 1200 s^{-1}. Step 1 and Step 2 are identical to that described above in relation to FIG. **1**. Once the sheet is formed with thickness from 1.2 mm to 10.0 mm, the sheet will then exhibit a total elongation of X_1 (%), an ultimate tensile strength of Y_1 (MPa), and a yield strength of Z_1 (MPa) when tested at strain rate S_1, which is preferably at or below 0.007 s^{-1} and in the range from 0.007 to 0.0001 s^{-1} Preferred properties for this alloy would be tensile elongation from 12 to 80%, ultimate tensile strength values from 700 to 2100 MPa, and yield strength is in a range from 250 to 1500 MPa. In Step 3, the sheet with thickness from 0.2 mm to less than 1.2 mm is such that when deformed at an engineering strain rate $S_2>S_1$ and the alloy exhibits $X_3=X_1\pm7\%$, ultimate tensile strength $Y_3=Y_1\pm200$ MPa, and yield strength $Z_3=Z_1\pm50$ MPa. The preferred properties of the alloy in Step 3 are as follows: X_3=5 to 87%; Y_3=500 MPa to 2300 MPa, and Z_3=200 MPa to 1550 MPa.

[0045] Alloys herein are also shown to avoid brittle fracture when stress concentration sites are introduced such as notches at the sheet edge. A stress concentration site herein is a location on the alloy sheet where stress can be concentrated, including but not limited to geometric discontinuities, such as a notch, hole, cut in the surface, crack, chipped portion, dent, etc. FIG. **3** shows a summary on how changes in mechanical properties are retained in the alloys herein with the introduction of stress concentration sites such as edge notches. Once the sheet is formed with thickness from 1.2 mm to 10.0 mm in Step 2, the sheet will then exhibit a total elongation of X_1 (%), an ultimate tensile strength of Y_1 (MPa), and a yield strength of Z_1 (MPa). Preferred properties for this alloy would again be tensile elongation from 12 to 80%, ultimate tensile strength values from 700 to 2100 MPa, and yield strength is in a range from 250 to 1500 MPa. In Step 3, the sheet that experiences a stress concentration is capable of exhibiting the following in response to a deformation: $X_4\geq0.2X_1$ (%), an ultimate tensile strength $Y_4\geq0.5Y_1$ (MPa), and a yield strength $Z_4\geq0.6Z_1$ (MPa). The preferred properties of the alloy in Step 3 are as follows: $X_4\geq2.4\%$; $Y_4\geq350$ MPa, and $Z_4\geq150$ MPa.

Alloys

[0046] The chemical composition of the alloys herein is shown in Table 1 which provides the preferred atomic ratios utilized.

TABLE 1

Chemical Composition of Alloys (Atomic %)							
Alloy	Fe	Cr	Ni	Mn	Si	Cu	C
Alloy 1	75.75	2.63	1.19	13.86	5.13	0.65	0.79
Alloy 2	74.75	2.63	1.19	14.86	5.13	0.65	0.79
Alloy 3	77.31	2.63	8.49	5.00	5.13	0.65	0.79
Alloy 4	77.14	2.63	6.49	7.17	5.13	0.65	0.79
Alloy 5	76.24	2.63	4.49	10.07	5.13	0.65	0.79
Alloy 6	75.34	2.63	2.49	12.97	5.13	0.65	0.79
Alloy 7	78.92	2.63	6.49	5.39	5.13	0.65	0.79
Alloy 8	77.34	2.63	4.49	8.97	5.13	0.65	0.79
Alloy 9	75.77	2.63	2.49	12.54	5.13	0.65	0.79
Alloy 10	75.90	2.63	3.74	11.16	5.13	0.65	0.79
Alloy 11	77.73	2.63	3.74	9.33	5.13	0.65	0.79
Alloy 12	79.57	2.63	3.74	7.49	5.13	0.65	0.79
Alloy 13	75.97	2.63	3.74	10.09	5.13	1.65	0.79
Alloy 14	77.80	2.63	3.74	8.26	5.13	1.65	0.79
Alloy 15	79.64	2.63	3.74	6.42	5.13	1.65	0.79
Alloy 16	76.88	2.63	3.74	9.18	5.13	1.65	0.79

TABLE 1-continued

Chemical Composition of Alloys (Atomic %)							
Alloy	Fe	Cr	Ni	Mn	Si	Cu	C
Alloy 17	76.83	2.63	3.74	9.85	5.13	1.03	0.79
Alloy 18	76.57	2.63	3.06	10.17	5.13	1.65	0.79
Alloy 19	76.52	2.63	3.06	10.84	5.13	1.03	0.79
Alloy 20	78.02	1.13	3.06	10.84	5.13	1.03	0.79
Alloy 21	80.02	1.13	3.06	10.84	3.13	1.03	0.79
Alloy 22	76.70	2.63	3.40	10.01	5.13	1.34	0.79
Alloy 23	76.20	3.13	3.40	10.01	5.13	1.34	0.79
Alloy 24	75.70	3.63	3.40	10.01	5.13	1.34	0.79
Alloy 25	77.70	2.63	3.40	10.01	4.13	1.34	0.79
Alloy 26	75.70	2.63	3.40	10.01	6.13	1.34	0.79
Alloy 27	77.20	2.63	3.40	10.01	4.13	1.34	1.29
Alloy 28	75.20	2.63	3.40	10.01	6.13	1.34	1.29
Alloy 29	76.98	2.88	3.40	10.01	4.63	1.34	0.76
Alloy 30	77.23	2.88	3.15	10.01	4.63	1.34	0.76
Alloy 31	77.48	2.88	2.90	10.01	4.63	1.34	0.76
Alloy 32	77.73	2.88	2.65	10.01	4.63	1.34	0.76
Alloy 33	77.98	2.88	2.40	10.01	4.63	1.34	0.76
Alloy 34	74.59	2.61	0.00	15.17	3.59	1.86	2.18
Alloy 35	82.22	3.69	9.94	0.00	2.26	0.37	1.52
Alloy 36	76.17	8.64	0.90	11.77	0.00	1.68	0.84
Alloy 37	82.77	4.41	6.66	3.19	1.14	1.16	0.67
Alloy 38	76.55	0.78	0.72	14.43	3.42	0.42	3.68
Alloy 39	81.44	0.00	4.42	10.33	2.87	0.00	0.94
Alloy 40	81.00	1.22	0.89	13.45	2.66	0.78	0.00
Alloy 41	81.68	2.24	3.25	9.87	0.00	1.55	1.41
Alloy 42	78.47	3.16	5.57	7.43	3.70	0.51	1.16
Alloy 43	79.73	3.34	7.02	4.95	3.22	0.46	1.28
Alloy 44	81.47	3.69	10.69	0.00	2.26	0.37	1.52
Alloy 45	80.72	3.69	11.44	0.00	2.26	0.37	1.52
Alloy 46	81.47	3.69	9.94	0.00	2.26	1.12	1.52
Alloy 47	80.72	3.69	9.94	0.00	2.26	1.87	1.52
Alloy 48	81.00	3.69	9.94	0.00	3.70	0.51	1.16
Alloy 49	82.84	1.85	9.94	0.00	3.70	0.51	1.16
Alloy 50	84.69	0.00	9.94	0.00	3.70	0.51	1.16
Alloy 51	82.30	3.69	4.97	3.67	3.70	0.51	1.16
Alloy 52	81.00	3.69	4.97	4.97	3.70	0.51	1.16
Alloy 53	79.70	3.69	4.97	6.27	3.70	0.51	1.16
Alloy 54	83.52	3.69	4.97	3.67	2.26	0.37	1.52
Alloy 55	82.22	3.69	4.97	4.97	2.26	0.37	1.52
Alloy 56	80.92	3.69	4.97	6.27	2.26	0.37	1.52

[0047] As can be seen from Table 1, the alloys herein comprise, consist essentially of, or consist of iron based metal alloys, having greater than 70 at. % Fe, and at least four or more elements selected from the following six (6) elements: Si, Mn, Cr, Ni, Cu, and C. The level of impurities of other elements are in the range of 0 to 5000 ppm. Accordingly, if there is 5000 ppm of an element other than the selected elements identified, the level of such selected elements may then in combination be present at a lower level to account for the 5000 ppm impurity, such that the total of all elements present (selected elements and impurities) is 100 atomic percent.

[0048] With regards to the above, and as can be further seen from Table 1, preferably, when Fe is present at a level of greater than 70 at. %, and one then selects the four or more elements from the indicated six (6) elements, or selects five or more elements, or selects all six elements to provide a formulation of elements that totals 100 atomic percent. The preferred levels of the elements, if selected, may fall in the following ranges: Si (1.14 to 6.13), Mn (3.19 to 15.17), Cr (0.78 to 8.64); Ni (0.9 to 11.44), Cu (0.37 to 1.87), and C (0.67 to 3.68). Accordingly, it can be appreciated that if four (4) elements are selected, two of the six elements are not selected and may be excluded. If five (5) elements are selected, one of the elements of the six can be excluded. Moreover, a particularly preferred level of Fe is in the range of 73.95 to 84.69 at. %. Again, the level of impurities of other elements are preferably controlled in the range of 0 to 5000 ppm (0 to 0.5 wt %).

Laboratory Slab Casting

[0049] Alloys were weighed out into 3,000 to 3,400 gram charges according to the atomic ratios in Table 1 using commercially available ferroadditive powders and a base steel feedstock with known chemistry. As alluded to above, impurities can be present at various levels depending on the feedstock used. Impurity elements would commonly include the following elements; Al, Co, N, P, Ti, Mo, W, Ga, Ge, Sb, Nb, Zr, O, Sn, Ca, and S which if present would be in the range from 0 to 5000 ppm (parts per million) (0 to 0.5 wt %) at the expense of the desired elements noted above. Preferably, the level of impurities is controlled to fall in the range of 0 to 3000 ppm (0.3 wt %).

[0050] Charges were loaded into a zirconia coated silica crucible which was placed into an Indutherm VTC800V vacuum tilt casting machine. The machine then evacuated the casting and melting chambers and flushed with argon to atmospheric pressure twice prior to casting to prevent oxidation of the melt. The melt was heated with a 14 kHz RF induction coil until fully molten, approximately from 5 to 7 minutes depending on the alloy composition and charge mass. After the last solids were observed to melt it was allowed to heat for an additional 30 to 45 seconds to provide superheat and ensure melt homogeneity. The casting machine then evacuated the chamber and tilted the crucible and poured the melt into a water cooled copper die. The melt was allowed to cool under vacuum for 200 seconds before the chamber was filled with argon to atmospheric pressure.

[0051] Laboratory casting corresponds to Step 1 in FIG. **1**, FIG. **2** and FIG. **3** and provides slabs with thickness of 50 mm. Depending on equipment capability, slab thickness in Step 1 can vary from 25.0 to 500 mm.

Thermal Analysis

[0052] A sample of between 50 and 150 mg from each alloy herein was taken in the as-cast condition. This sample was heated to an initial ramp temperature between 900° C. and 1300° C. depending on alloy chemistry, at a rate of 40° C./min. Temperature was then increased at 10° C./min to a max temperature between 1425° C. and 1515° C. depending on alloy chemistry. Once this maximum temperature was achieved, the sample was cooled at a rate of 10° C./min back to the initial ramp temperature before being reheated at 10° C./min to the maximum temperature. Differential Scanning calorimetry (DSC) measurements were taken using a Netzsch Pegasus 404 DSC through all four stages of the experiment, and this data was used to determine the solidus and liquidus temperatures of each alloy, which are in a range from 1102 to 1505° C. (Table 2). Depending on alloys chemistry, liquidus-solidus gap varies from 31 to 138° C. Thermal analysis provides information on maximum temperature for the following hot rolling processes that varies depending on alloy chemistry.

TABLE 2

Thermal Analysis of Selected Alloys

Alloy	Solidus (° C.)	Liquidus (° C.)	Melting Gap (° C.)
Alloy 1	1390	1448	58
Alloy 2	1398	1446	49
Alloy 3	1403	1456	53
Alloy 4	1411	1456	45
Alloy 5	1391	1448	57
Alloy 6	1384	1442	58
Alloy 7	1407	1462	55
Alloy 8	1400	1452	52
Alloy 9	1386	1444	59
Alloy 10	1375	1444	70
Alloy 11	1392	1453	61
Alloy 12	1393	1459	67
Alloy 13	1374	1441	67
Alloy 14	1386	1453	67
Alloy 15	1401	1459	57
Alloy 16	1400	1453	53
Alloy 17	1397	1453	56
Alloy 18	1399	1452	53
Alloy 19	1400	1452	52
Alloy 20	1401	1454	53
Alloy 21	1409	1467	57
Alloy 22	1396	1452	56
Alloy 23	1394	1450	56
Alloy 24	1404	1454	49
Alloy 25	1405	1460	55
Alloy 26	1372	1440	68
Alloy 27	1383	1454	70
Alloy 28	1369	1430	61
Alloy 29	1420	1458	38
Alloy 30	1412	1459	47
Alloy 31	1431	1462	31
Alloy 32	1408	1460	52
Alloy 33	1415	1462	48
Alloy 34	1358	1445	88
Alloy 35	1458	1496	39
Alloy 36	1406	1488	82
Alloy 37	1462	1502	41
Alloy 38	1294	1432	138
Alloy 39	1438	1491	53
Alloy 40	1425	1481	56
Alloy 41	1438	1494	56
Alloy 42	1442	1481	39
Alloy 43	1460	1493	33
Alloy 44	1458	1500	42
Alloy 45	1465	1505	39
Alloy 46	1456	1498	42
Alloy 47	1453	1492	39
Alloy 48	1456	1496	40
Alloy 49	1472	1504	32
Alloy 50	1456	1500	43
Alloy 51	1451	1491	40
Alloy 52	1430	1480	51
Alloy 53	1442	1482	40
Alloy 54	1447	1489	42
Alloy 55	1450	1490	40
Alloy 56	1447	1488	41

Laboratory Hot Rolling

[0053] The alloys herein were preferably processed into a laboratory hot band by hot rolling of laboratory slabs at high temperatures. Laboratory alloy processing is developed to simulate the hot band production from slabs produced by continuous casting. Industrial hot rolling is performed by heating a slab in a tunnel furnace to a target temperature, then passing it through either a reversing mill or a multi-stand mill or a combination of both to reach the target gauge. During rolling on either mill type, the temperature of the slab is steadily decreasing due to heat loss to the air and to the work rolls so the final hot band is formed at a reduced temperature. This is simulated in the laboratory by heating in a tunnel furnace to between 1100° C. and 1250° C., then hot rolling. The laboratory mill is slower than industrial mills causing greater loss of heat during each hot rolling pass so the slab is reheated for 4 minutes between passes to reduce the drop in temperature, the final temperature at target gauge when exiting the laboratory mill commonly is in the range from 800° C. to 1000° C., depending on furnace temperature and final thickness.

[0054] Prior to hot rolling, laboratory slabs were preheated in a Lucifer EHS3GT-B18 furnace. The furnace set point varies between 1100° C. to 1250° C., depending on alloy melting point and point in the hot rolling process, with the initial temperatures set higher to facilitate higher reductions, and later temperatures set lower to minimize surface oxidation on the hot band. The slabs were allowed to soak for 40 minutes prior to hot rolling to ensure they reach the target temperature and then pushed out of the tunnel furnace into a Fenn Model 061 2 high rolling mill. The 50 mm casts are hot rolled for 5 to 10 passes though the mill before being allowed to air cool. Final thickness ranges after hot rolling are preferably from 1.8 mm to 4.0 mm with variable reduction per pass ranging from 20% to 50%.

[0055] Tensile specimens were cut from laboratory hot band using wire EDM. Tensile properties were measured on an Instron mechanical testing frame (Model 3369), utilizing Instron's Bluehill control and analysis software. Samples were tested under displacement control at a constant displacement rate of 0.036 mm/s, which resulted in sample strain rates, calculated from video strain measurements, ranging from 4.4×10^{-4} s^{-1} to 6.8×10^{-3} s^{-1}, depending on several factors including, but not always limited to mechanical compliance, sample slippage, and settling of the wedge action grips used.

[0056] Tensile properties of the alloys in the hot rolled condition with a thickness from 1.8 to 2.3 mm are listed in Table 3 including magnetic phases volume percent (Fe %) that was measured by Feritscope. The ultimate tensile strength values may vary from 913 to 2011 MPa with tensile elongation from 13.0 to 69.5%. The yield strength is in a range from 250 to 1313 MPa. Mechanical properties of the hot band from steel alloys herein depend on alloy chemistry, processing conditions, and material mechanistic response to the processing conditions. The relative magnetic phases volume percent was measured by Feritscope with the magnetic phases volume percent of 0.1 to 64.9 Fe % in a hot band depending on alloy chemistry. Note that the Table 3 properties correspond to Step 2 of FIG. **1**, FIG. **2**, and FIG. **3**. Further processing of the hot band can additionally occur through cold rolling and annealing as shown for example in Case Example 1.

TABLE 3

Hot Band Tensile Properties of Alloys

Alloy	Tensile Elongation (%)	Ultimate Tensile Strength (MPa)	Yield Strength (MPa)	Average Magnetic Phases Volume Percent (Fe %)
Alloy 1	51.4	1248	294	1.7
	49.2	1253	310	
	31.2	1093	396	

TABLE 3-continued

Hot Band Tensile Properties of Alloys

Alloy	Tensile Elongation (%)	Ultimate Tensile Strength (MPa)	Yield Strength (MPa)	Average Magnetic Phases Volume Percent (Fe %)
Alloy 2	57.6	1175	311	1.3
	58.6	1209	294	
	56.6	1167	302	
Alloy 3	55.4	1163	330	3.2
	59.5	1154	373	
	58.1	1165	347	
Alloy 4	59.8	1220	342	0.3
	51.6	1241	338	
	55.5	1245	375	
	54.6	1324	377	
Alloy 5	54.3	1248	325	0.5
	53.1	1218	313	
	50.6	1258	304	
	54.1	1242	331	
Alloy 6	58.3	1212	330	0.4
	53.7	1212	283	
	58.7	1193	315	
Alloy 7	28.1	1508	333	10.4
	28.5	1516	331	
	26.0	1520	317	
Alloy 8	41.2	1343	330	0.9
	32.8	1281	328	
	45.7	1387	336	
	41.4	1375	328	
Alloy 9	48.1	1248	300	1.4
	50.5	1293	304	
	52.0	1280	303	
Alloy 10	58.5	1229	379	2.7
	57.8	1223	384	
	59.0	1220	389	
Alloy 11	45.3	1411	360	0.8
	40.2	1460	359	
	41.3	1429	325	
	47.1	1448	347	
Alloy 12	31.3	1624	250	1.5
	31.7	1581	304	
	28.7	1610	319	
Alloy 13	57.1	1101	358	0.1
	66.1	1120	362	
	68.5	1114	362	
	60.1	1120	350	
Alloy 14	45.1	1371	354	0.4
	40.6	1403	363	
	42.3	1403	364	
	46.9	1379	341	
Alloy 15	26.2	1579	295	1.6
	25.2	1593	264	
	24.6	1588	302	
Alloy 16	54.8	1239	379	0.2
	58.5	1207	341	
	55.8	1207	359	
Alloy 17	51.3	1270	354	0.6
	50.1	1328	384	
Alloy 18	58.8	1224	384	0.3
	56.1	1245	390	
	50.7	1190	365	
Alloy 19	47.4	1263	348	0.4
	50.7	1260	362	
	51.8	1277	363	
Alloy 20	40.1	1337	376	0.3
	43.9	1343	375	
	44.7	1328	394	
Alloy 21	45.2	1277	327	0.5
	46.1	1318	340	
	54.2	1310	325	
Alloy 22	49.6	1272	369	0.3
	54.9	1275	354	
	54.8	1271	319	
	52.4	1297	340	

TABLE 3-continued

Hot Band Tensile Properties of Alloys				
Alloy	Tensile Elongation (%)	Ultimate Tensile Strength (MPa)	Yield Strength (MPa)	Average Magnetic Phases Volume Percent (Fe %)
Alloy 23	53.5	1246	344	0.3
	55.9	1226	359	
	51.2	1232	346	
	52.7	1228	375	
Alloy 24	57.0	1209	356	0.2
	54.6	1202	348	
	55.1	1207	363	
	56.9	1225	338	
Alloy 25	53.4	1227	357	0.4
	56.5	1249	325	
	54.5	1214	345	
	49.5	1220	343	
Alloy 26	49.0	1319	340	0.5
	48.4	1320	344	
	50.5	1304	331	
	51.1	1296	346	
Alloy 27	56.5	967	404	0.1
	54.5	956	421	
	67.6	979	417	
	52.0	942	390	
Alloy 28	50.4	1121	442	0.4
	49.8	1088	407	
	51.8	1116	423	
Alloy 29	56.0	1229	422	4.2
	56.3	1247	409	
	54.6	1226	405	
	50.0	1196	421	
	56.3	1199	412	
	53.3	1205	402	
Alloy 30	52.1	1271	421	5.5
	51.4	1284	416	
	50.6	1269	407	
	53.9	1248	418	
	49.9	1237	399	
	54.8	1241	407	
Alloy 31	48.6	1326	379	6.5
	51.3	1323	390	
	51.6	1293	372	
	51.4	1314	374	
Alloy 32	49.5	1347	383	5.7
	47.0	1367	388	
	47.9	1341	381	
	47.8	1391	431	
Alloy 33	44.8	1373	372	7.3
	42.3	1392	381	
	40.7	1388	381	
Alloy 34	65.9	963	515	0.3
	58.7	954	485	
	62.1	970	545	
Alloy 35	19.6	2000	533	43.3
	22.3	1976	511	
	19.8	1995	526	
Alloy 36	60.1	1091	439	2.0
	61.0	1114	469	
	59.4	1137	481	
Alloy 37	13.8	1572	649	56.4
	14.1	1619	711	
	14.6	1610	692	
Alloy 38	58.9	1105	531	0.7
	61.4	1108	524	
	58.6	1106	511	
Alloy 39	51.0	1317	354	8.2
	50.5	1334	370	
	50.5	1325	368	
Alloy 40	47.9	1374	330	5.8
	48.8	1336	317	
	41.5	1362	321	
Alloy 41	51.1	963	472	5.2
	48.4	913	463	

TABLE 3-continued

Hot Band Tensile Properties of Alloys				
Alloy	Tensile Elongation (%)	Ultimate Tensile Strength (MPa)	Yield Strength (MPa)	Average Magnetic Phases Volume Percent (Fe %)
Alloy 42	61.6	1081	440	7.0
	69.5	1098	450	
	64.3	1070	440	
	67.2	1081	438	
	62.2	1082	439	
Alloy 43	44.5	1176	440	16.6
	35.0	1073	447	
	38.4	1136	447	
	36.8	1140	454	
Alloy 44	23.9	1858	577	40.5
	24.5	1852	624	
	24.9	1866	685	
	23.1	1841	672	
Alloy 45	32.5	1758	439	32.4
	28.9	1733	408	
	26.9	1746	442	
	26.6	1725	417	
Alloy 46	21.9	1917	826	46.0
	21.4	1898	753	
	21.0	1907	748	
	22.2	1911	698	
Alloy 47	24.8	1765	526	40.1
	24.6	1787	492	
	23.7	1781	463	
	24.2	1771	478	
Alloy 48	16.2	1890	1108	55.0
	17.0	1926	1093	
	15.9	1920	1139	
	16.4	1899	1073	
Alloy 49	16.4	2002	1247	61.5
	15.4	1961	1225	
	16.0	2011	1276	
	16.3	1990	1275	
Alloy 50	16.9	1853	1259	64.9
	15.4	1859	1265	
	15.7	1816	1195	
	14.6	1833	1313	
Alloy 51	18.8	1960	944	51.8
	17.8	1963	911	
	18.1	1947	994	
	17.3	1915	927	
Alloy 52	23.3	1598	366	24.5
	20.1	1522	369	
	25.4	1627	364	
	25.6	1624	383	
Alloy 53	40.3	1407	447	13.1
	37.6	1375	441	
	37.6	1310	437	
	41.2	1393	444	
Alloy 54	19.0	1834	416	36.4
	17.8	1827	420	
	13.0	1720	423	
	15.4	1811	462	
Alloy 55	23.0	1237	462	24.9
	18.3	1088	443	
	21.6	1212	468	
	22.9	1302	470	
Alloy 56	36.8	1039	473	13.2
	36.0	1051	497	
	36.4	1026	480	
	34.9	1068	514	

CASE EXAMPLES

Case Example #1 Tensile Properties of the Sheet at 1.2 mm Thickness

[0057] The hot band from alloys herein listed in Table 1 was cold rolled to final target gauge thickness of 1.2 mm through multiple cold rolling passes. Cold rolling is defined as rolling at ambient temperature. Hot band material was media blasted prior to cold rolling to remove surface oxides which could become embedded during the rolling process. The resultant cleaned sheet material was rolled using a Fenn Model 061 2 high rolling mill. Sheet was fed through the rolls, and the roll gap is reduced for each subsequent pass until the desired thickness is achieved or the material hardens to the point where additional rolling does not achieve significant reduction in thickness. Annealing was applied before next rolling to recover ductility. Multiple cycles of cold rolling and annealing might be applied. Once the final gauge thickness was reached, samples were cut from each cold rolled sheet by wire EDM. Tensile properties were measured on an Instron mechanical testing frame (Model 3369), utilizing Instron's Bluehill control and analysis software. All tests were run at ambient temperature in displacement control. Samples were tested under displacement control at a constant displacement rate of 0.036 mm/s, which resulted in sample strain rates, calculated from video strain measurements, ranging from 4.4×10^{-4} s^{-1} to 6.8×10^{-3} s^{-1}, depending on several factors including, but not always limited to mechanical compliance, sample slippage, and settling of the wedge action grips used.

[0058] Tensile properties of 1.2 mm thick sheet from alloys herein after cold rolling are listed in Table 4. The ultimate tensile strength values after cold rolling is in a range from 1360 to 2222 MPa; yield strength varies from 1006 to 2073 MPa and tensile elongation is recorded in the range from 4.2 to 37.2%. The magnetic phases volume percent was measured by Feritscope in a range from 1.6 to 84.9 Fe % in a cold rolled sheet depending on alloy chemistry.

TABLE 4

Tensile Properties of 1.2 mm Thick Sheet from the Alloys After Cold Rolling

Alloy	Tensile Elongation (%)	Ultimate Tensile Strength (MPa)	Yield Strength (MPa)	Magnetic Phases Volume Percent (Fe %)	Cold Rolling Reduction (%)
Alloy 1	20.5	1712	1114	31.4	38.0
	20.4	1712	1131		
	15.0	1705	1073		
Alloy 2	21.8	1603	1135	27.8	39.7
	23.2	1612	1111		
	25.7	1589	1120		
Alloy 3	29.9	1540	1140	34.6	36.9
	28.9	1551	1118		
	29.5	1553	1234		
Alloy 4	25.4	1645	1192	43.3	39.2
	25.6	1650	1217		
	26.4	1639	1381		
Alloy 5	17.1	1758	1335	44.9	38.3
	18.5	1764	1321		
	17.8	1764	1285		
Alloy 6	22.5	1686	1018	31.3	35.3
	22.9	1685	1072		
	21.6	1687	1042		
Alloy 7	16.9	1874	1666	66.5	35.7
	14.8	1881	1680		
	13.3	1875	1360		
Alloy 8	10.7	1835	1068	53.4	35.4
	16.4	1859	1086		
	17.5	1860	1336		
Alloy 9	19.7	1742	1014	37.0	36.0
	17.5	1732	1104		
	18.2	1732	1120		

TABLE 4-continued

Tensile Properties of 1.2 mm Thick Sheet from the Alloys After Cold Rolling

Alloy	Tensile Elongation (%)	Ultimate Tensile Strength (MPa)	Yield Strength (MPa)	Magnetic Phases Volume Percent (Fe %)	Cold Rolling Reduction (%)
Alloy 10	20.1	1715	1038	40.3	35.1
	20.5	1716	1280		
	20.5	1729	1173		
Alloy 11	13.9	1893	1320	69.9	32.7
	15.0	1906	1467		
	15.6	1875	1536		
Alloy 12	5.5	2125	1913	57.0	33.8
	5.9	2116	1720		
	4.2	2114	1675		
Alloy 13	22.8	1500	1182	25.6	36.5
	24.0	1523	1204		
	23.9	1518	1098		
Alloy 14	18.6	1790	1561	52.1	34.5
	20.2	1793	1436		
	17.9	1726	1491		
Alloy 15	5.0	2051	1784	58.9	37.3
	6.2	2073	2000		
	6.3	2057	1957		
Alloy 16	19.9	1700	1413	42.0	36.9
	19.7	1689	1436		
	21.1	1704	1302		
Alloy 17	20.1	1765	1379	45.9	36.0
	20.2	1759	1306		
	17.2	1764	1374		
Alloy 18	20.6	1708	1388	44.1	37.3
	20.0	1721	1326		
	18.9	1709	1369		
Alloy 19	18.9	1810	1213	44.8	38.0
	19.3	1807	1324		
	19.2	1806	1260		
Alloy 20	15.1	1864	1404	54.8	38.3
	16.2	1884	1461		
	17.1	1879	1512		
Alloy 21	18.6	1780	1374	54.9	34.1
	18.0	1785	1414		
	18.6	1786	1006		
Alloy 22	17.3	1759	1356	43.9	38.0
	21.3	1736	1196		
	18.8	1757	1304		
Alloy 23	19.3	1718	1240	41.3	37.4
	20.4	1728	1283		
	19.0	1727	1271		
Alloy 24	22.0	1709	1136	36.8	37.5
	12.6	1695	1256		
	14.8	1706	1258		
Alloy 25	19.8	1715	1326	42.6	33.5
	20.2	1704	1320		
	21.0	1700	1316		
Alloy 26	18.8	1822	1377	48.5	35.6
	17.9	1816	1327		
Alloy 27	30.7	1442	1146	12.6	34.5
	29.9	1360	1108		
	24.2	1428	1164		
Alloy 28	21.0	1625	1215	20.6	37.5
	26.6	1646	1187		
	23.9	1602	1172		
Alloy 29	18.1	1718	1483	58.3	38.8
	18.6	1712	1454		
	19.4	1720	1407		
Alloy 30	17.7	1770	1335	44.6	39.9
	17.7	1764	1430		
	17.9	1765	1515		
Alloy 31	17.5	1834	1524	49.4	40.5
	16.9	1831	1707		
	16.0	1837	1578		
Alloy 32	15.7	1890	1442	50.2	41.1
	14.8	1897	1563		
	15.4	1886	1676		

TABLE 4-continued

Tensile Properties of 1.2 mm Thick Sheet from the Alloys After Cold Rolling

Alloy	Tensile Elongation (%)	Ultimate Tensile Strength (MPa)	Yield Strength (MPa)	Magnetic Phases Volume Percent (Fe %)	Cold Rolling Reduction (%)
Alloy 33	15.4	1891	1533	56.3	38.2
	16.3	1889	1604		
	15.8	1895	1419		
Alloy 34	10.9	1519	1249	1.6	39.0
	9.4	1515	1037		
	10.8	1519	1345		
Alloy 35*	16.2	2222	1693	73.7	19.6
	16.4	2216	1735		
	16.2	2217	1657		
Alloy 36	16.4	1641	1116	29.6	36.7
	20.6	1604	1187		
	19.1	1623	1295		
Alloy 37	7.1	1949	1617	84.9	36.3
	6.6	1977	1824		
	6.5	1975	1834		
Alloy 38	7.0	1727	1539	3.8	43.0
	9.7	1721	1373		
	10.0	1717	1490		
Alloy 39	16.0	1869	1289	50.0	36.5
	19.0	1840	1471		
	19.0	1837	1245		
Alloy 40	15.6	1917	1238	45.8	37.4
	17.2	1913	1361		
	17.7	1917	1192		
Alloy 41	28.6	1452	1121	26.4	39.2
	31.1	1445	1101		
	31.1	1431	1231		
Alloy 42	21.4	1673	1516	35.5	44.9
	23.1	1686	1519		
	22.9	1675	1509		
Alloy 43	37.2	1656	1313	38.1	39.2
	31.2	1650	1304		
	30.0	1667	1332		
Alloy 44	19.6	2091	1623	57.8	37.1
	20.4	2095	1653		
	20.1	2098	1656		
Alloy 45	21.7	2028	1331	50.9	40.9
	22.8	2014	1313		
	22.6	2017	1334		
Alloy 46*	18.5	2095	1755	62.2	29.3
	18.5	2100	1754		
	19.3	2106	1773		
Alloy 47	14.7	2024	1482	57.8	36.2
	21.3	2020	1496		
	19.4	2024	1473		
Alloy 48*	11.7	2197	2029	72.6	20.7
	11.6	2197	1993		
	10.6	2197	2010		
Alloy 49	11.1	2138	1985	76.6	11.3
	11.6	2137	1948		
	11.1	2138	1964		
Alloy 50*	8.7	2166	2041	83.3	26.7
	8.0	2168	2060		
	8.5	2170	2073		
Alloy 51*	11.9	2197	1904	68.4	21.0
	11.0	2194	1917		
	12.0	2190	1897		
Alloy 52	15.2	2071	1788	55.1	34.6
	16.4	2068	1764		
	13.8	2073	1781		
Alloy 53	22.1	1908	1630	45.3	38.5
	23.5	1911	1584		
	24.3	1908	1590		
Alloy 54*	7.9	2104	1675	57.5	30.3
	5.8	2032	1673		
	7.4	2083	1646		
Alloy 55	8.2	1738	1479	44.5	38.1
	11.0	1812	1497		
	11.5	1829	1486		
Alloy 56	28.8	1705	1386	32.9	39.4
	32.5	1703	1452		
	28.2	1747	1443		

*Thickness of 1.2 mm was not achieved in these alloys due to high strength and equipment limitations. Alloys are tested at thickness from 1.3 to 1.4 mm.

[0059] The samples were annealed under conditions intended to simulate the thermal exposure expected during an industrial continuous annealing process representing final treatment of sheet material in Step 2 in FIG. **1**, FIG. **2** and FIG. **3**. Samples were loaded into a furnace preheated to 850° C., and held at temperature for 10 minutes, wrapped in foil and held under a steady argon flow to minimize oxidation damage. Samples were removed at temperature and allowed to air cool to ambient temperature before testing. Tensile properties were measured on an Instron mechanical testing frame (Model 3369), utilizing Instron's Bluehill control and analysis software. All tests were run at ambient temperature in displacement control at a constant displacement rate of 0.036 mm/s, which resulted in sample strain rates, calculated from video strain measurements, ranging from 4.4×10^{-4} s^{-1} to 6.8×10^{-3} s^{-1}, depending on several factors including, but not always limited to mechanical compliance, sample slippage, and settling of the wedge action grips used.

[0060] Tensile properties of 1.2 mm sheet from alloys herein after annealing are listed in Table 5. The ultimate tensile strength values of the annealed sheet from alloys herein is in a range from 725 to 2072 MPa; yield strength varies from 267 to 1428 MPa and tensile elongation is recorded in the range from 12.8 to 76.9%. The relative magnetic phases volume percent was measured by Feritscope with the magnetic phases volume percent of 0.2 to 68.2 Fe % depending on alloy chemistry.

[0061] Properties of cold rolled and annealed sheet from Alloys herein corresponds to Step 2 in FIG. **1**, FIG. **2** and FIG. **3**.

TABLE 5

Tensile Properties of 1.2 mm Thick Sheet from the Alloys after Annealing

Alloy	Tensile Elongation (%)	Ultimate Tensile Strength (MPa)	Yield Strength (MPa)	Average Magnetic Phases Volume Percent (Fe %)
Alloy 1	55.7	1267	473	1.2
	52.0	1242	451	
	56.1	1248	470	
	57.7	1277	463	
Alloy 2	62.4	1162	491	1.3
	59.4	1179	469	
	61.8	1193	477	
	62.6	1172	531	
Alloy 3	61.2	1165	319	0.9
	64.2	1153	320	
	63.2	1145	302	
Alloy 4	61.9	1218	350	1.2
	58.6	1201	344	

TABLE 5-continued

Tensile Properties of 1.2 mm Thick Sheet from the Alloys after Annealing

Alloy	Tensile Elongation (%)	Ultimate Tensile Strength (MPa)	Yield Strength (MPa)	Average Magnetic Phases Volume Percent (Fe %)
	51.4	1223	341	
	64.1	1208	337	
Alloy 5	52.0	1239	393	0.7
	54.6	1235	398	
	53.9	1227	442	
Alloy 6	61.3	1194	426	1.0
	61.0	1238	450	
	53.9	1208	417	
Alloy 7	31.5	1440	338	10.8
	33.1	1475	322	
	32.7	1483	312	
	33.1	1481	347	
	31.3	1461	323	
	32.1	1472	332	
Alloy 8	56.2	1269	430	0.9
	61.3	1225	471	
	56.6	1277	421	
Alloy 9	56.2	1269	430	1.0
	61.3	1225	471	
	56.6	1277	421	
Alloy 10	54.3	1238	412	0.7
	56.9	1192	397	
	59.9	1238	412	
Alloy 11	41.3	1437	420	0.9
	44.3	1434	424	
	41.7	1464	412	
	43.5	1419	417	
Alloy 12	29.9	1574	379	2.3
	30.1	1571	374	
	29.7	1579	373	
Alloy 13	62.9	1097	367	1.0
	69.8	1121	375	
	68.9	1103	368	
Alloy 14	47.1	1363	372	1.1
	46.7	1384	376	
	43.8	1365	366	
	42.6	1386	370	
Alloy 15	24.2	1528	305	20.0
	24.8	1535	308	
	26.0	1534	315	
Alloy 16	54.6	1243	376	0.9
	55.0	1258	422	
	54.8	1237	376	
	55.9	1249	382	
Alloy 17	53.3	1333	406	0.4
	50.0	1304	410	
	53.6	1289	403	
	51.1	1323	392	
Alloy 18	55.2	1238	420	0.6
	58.7	1198	414	
	56.1	1235	425	
	53.2	1244	417	
Alloy 19	50.4	1273	451	0.8
	50.5	1278	416	
	51.0	1348	436	
	53.2	1299	414	
Alloy 20	43.4	1378	408	1.0
	44.7	1362	406	
	34.1	1308	429	
	28.7	1175	397	
Alloy 21	52.7	1298	340	1.6
	46.9	1326	348	
	35.4	1270	349	
	48.6	1324	350	
Alloy 22	54.8	1273	399	0.9
	54.1	1268	397	
	56.1	1297	408	
Alloy 23	59.3	1239	403	0.3
	59.5	1296	407	
	56.2	1255	409	

TABLE 5-continued

Tensile Properties of 1.2 mm Thick Sheet from the Alloys after Annealing

Alloy	Tensile Elongation (%)	Ultimate Tensile Strength (MPa)	Yield Strength (MPa)	Average Magnetic Phases Volume Percent (Fe %)
Alloy 24	60.0	1235	423	0.7
	60.1	1247	432	
	61.8	1237	428	
Alloy 25	56.8	1255	376	0.3
	51.6	1244	380	
	57.0	1217	382	
Alloy 26	51.0	1305	417	0.7
	50.0	1311	432	
	51.1	1319	433	
Alloy 27	59.7	1033	387	0.5
	53.8	975	368	
	63.0	1017	377	
Alloy 28	41.3	1128	480	0.2
	45.7	1168	482	
	47.2	1168	485	
	47.0	1168	492	
Alloy 29	58.4	1218	370	1.1
	50.7	1250	386	
	57.3	1251	378	
	55.1	1239	382	
Alloy 30	49.0	1297	383	1.1
	54.0	1318	445	
	53.3	1304	381	
Alloy 31	45.0	1299	382	1.2
	47.5	1328	383	
	52.3	1328	392	
	50.8	1328	397	
Alloy 32	50.9	1380	420	1.1
	43.1	1373	391	
	52.4	1371	390	
Alloy 33	45.6	1399	388	1.1
	36.3	1383	396	
	44.2	1418	398	
	34.4	1380	410	
Alloy 34	64.7	993	484	0.3
	66.1	997	491	
	66.2	994	481	
	66.3	994	491	
Alloy 35*	14.0	2066	792	60.1
	14.0	2072	775	
	14.5	2072	745	
	13.6	1971	775	
Alloy 36	50.1	1175	483	0.9
	50.9	1161	472	
	50.8	1190	471	
Alloy 37	13.2	1621	635	68.2
	13.2	1607	645	
	13.5	1586	574	
	13.4	1600	644	
Alloy 38	60.3	1134	499	0.5
	58.2	1141	500	
	60.4	1139	500	
	64.2	1138	490	
Alloy 39	20.2	929	372	3.0
	16.2	725	375	
	19.4	827	382	
	21.9	941	362	
Alloy 40	15.6	759	379	0.6
	17.9	888	420	
	17.0	839	368	
	18.0	849	431	
Alloy 41	53.0	889	312	1.4
	43.5	893	311	
	50.9	882	315	
Alloy 42	68.5	1126	381	1.4
	74.7	1105	370	
	75.2	1154	384	
	76.9	1141	375	
Alloy 43	51.3	1285	344	3.0
	50.6	1296	352	

TABLE 5-continued

Tensile Properties of 1.2 mm Thick Sheet from the Alloys after Annealing

Alloy	Tensile Elongation (%)	Ultimate Tensile Strength (MPa)	Yield Strength (MPa)	Average Magnetic Phases Volume Percent (Fe %)
	41.2	1132	341	
	62.4	1284	342	
Alloy 44	12.8	1898	1269	57.5
	14.0	1959	1272	
	14.1	1962	808	
	14.1	1961	1235	
Alloy 45	16.1	1875	540	51.3
	15.5	1888	517	
	16.0	1867	514	
	15.4	1878	546	
Alloy 46*	14.2	2007	1125	59.0
	14.3	2004	879	
	14.6	1998	866	
	13.5	2000	903	
Alloy 47	13.3	1888	1217	53.6
	14.6	1877	1240	
	13.0	1884	1237	
	14.2	1892	1253	
Alloy 48*	15.2	1853	1128	59.1
	15.0	1854	1130	
	15.4	1852	1131	
Alloy 49	15.3	1982	1409	65.1
	15.6	1998	1399	
	14.2	1964	1381	
	15.4	2008	1428	
Alloy 50*	14.6	1833	1307	64.8
	14.7	1846	1325	
	14.5	1844	1271	
	14.4	1844	1387	
Alloy 51*	15.9	1940	1297	57.5
	15.4	1937	1209	
	16.0	1929	1223	
Alloy 52	25.4	1722	314	23.2
	24.6	1719	267	
	23.8	1706	276	
	28.6	1717	319	
Alloy 53	47.3	1492	421	5.0
	44.1	1514	420	
	38.4	1478	401	
	48.9	1488	420	
Alloy 54*	17.7	2012	569	50.8
	17.1	2009	1053	
	17.0	2017	1158	
	16.8	2023	1140	
Alloy 55	35.0	1627	351	20.6
	39.6	1656	350	
	33.0	1657	358	
Alloy 56	42.2	1265	388	6.4
	41.2	1288	391	
	45.9	1345	395	
	47.7	1289	387	

*Thickness of 1.2 mm was not achieved in these alloys due to high strength and equipment limitations.
Samples were tested at thickness from 1.3 to 1.4 mm.

[0062] This Case Example demonstrates properties of the sheet material from alloys herein with thickness of 1.2 to 1.4 mm and tested at strain rates from 4.4×10^{-4} s^{-1} to 6.8×10^{-3} s^{-1}.

Case Example #2 Sheet Thickness Effect on Tensile Properties of Alloy 2

[0063] The hot band from Alloy 2 was cold rolled into sheets with different thicknesses through multiple cold rolling passes. Once the targeted gauge thickness was reached, samples were cut from each cold rolled sheet by wire EDM. The samples were annealed under conditions intended to simulate the thermal exposure expected during an industrial continuous annealing process. Samples were wrapped in stainless steel foil to prevent oxidation and loaded into a preheated furnace at 850° C. Samples were left in the furnace for 10 minutes while the furnace purged with argon before being removed and allowed to air cool. The only exception was the final anneal for the 4.8 mm material. This anneal was an 850° C. 20 min air cooled anneal, as opposed to the 10 minute anneal used for every other thickness. The purpose of this change was to allow more time for the material to heat up as it was a much thicker sample. Tensile properties were measured on an Instron mechanical testing frame (Model 5984), utilizing Instron's Bluehill control and analysis software. All tests were run at ambient temperature in displacement control. All samples were tested at displacement rate of 0.125 mm/s, which resulted in sample strain rates, calculated from video strain measurements, ranging from 9.1×10^{-4} s^{-1} to 1.9×10^{-3} s^{-1} depending on several factors including, but not always limited to mechanical compliance, sample slippage, and settling of the wedge action grips used.

[0064] The results of tensile testing of the sheet from Alloy 2 processed to different thicknesses are listed in Table 6. In samples with thickness less than 1.2 mm representing Step 3 in FIG. **1**, tensile strength varies from 1100 to 1190 MPa and yield strength is between 408 and 439 MPa. FIG. **4** and FIG. **5** show the tensile properties of Alloy 2 sheet as a function of the thickness. Average tensile elongation is 53.7% for Alloy 2 sheet with thickness varying from 0.20 to 1.03 mm (as compared to average of 61.5% in Alloy 2 sheet with thickness of 1.2 mm). Slightly higher elongation is observed up to 66.4% in thicker sheet samples above 1.2 mm. The stress-strain curves in FIG. **6** also demonstrate consistent properties and stress-strain behavior in sheet samples with different thicknesses.

TABLE 6

Sheet Thickness Effect on Tensile Properties of Alloy 2

Sample Thickness (mm)	Tensile Elongation (%)	Ultimate Tensile Strength (MPa)	Yield Strength (MPa)
4.82	54.7	1164	377
4.81	60.2	1202	380
4.79	57.8	1203	350
3.05	57.5	1222	453
3.04	66.4	1183	462
3.01	65.8	1190	450
1.03	52.3	1190	411
1.03	53.8	1179	410
1.02	62.1	1170	408
1.00	57.6	1186	415
0.77	54.8	1184	432
0.77	53.8	1178	430
0.75	52.2	1180	428
0.53	55.3	1148	417
0.53	53.5	1106	423
0.53	51.7	1163	422
0.41	51.6	1111	438
0.41	53.9	1120	439
0.41	51.1	1100	439
0.21	51.2	1125	434
0.20	51.0	1124	434

[0065] This Case Example demonstrates that high ductility maintained in the sheet with thickness in a wide range from 4.8 mm down to as small as 0.2 mm. Reduction in sheet thickness below 1.2 mm results in an average total elongation that is no less than that in the sheet with 1.2 mm thickness and above minus 7.8%. An average ultimate tensile strength is 25 MPa less than that in the corresponding sheet with 1.2 mm thickness and above and average yield strength is 67 MPa less.

Case Example #3 Thickness Effect on Tensile Properties of Sheet from Selected Alloys

[0066] The hot band from Alloy 1, Alloy 27, and Alloy 37 was cold rolled in to sheets with different thicknesses less than 1.2 mm through multiple cold rolling passes. Once the targeted gauge thickness was reached, samples were cut from each cold rolled sheet by wire EDM. The samples were annealed under conditions intended to simulate the thermal exposure expected during an industrial continuous annealing process representing final treatment at sheet processing in Step 2 in FIG. **1**. Samples were wrapped in stainless steel foil to prevent oxidation and loaded into a preheated furnace at 850° C. Samples were left in the furnace to 10 minutes while the furnace purged with argon before being removed and allowed to air cool. Tensile properties were measured on an Instron mechanical testing frame (Model 5984), utilizing Instron's Bluehill control and analysis software. All tests were run at ambient temperature in displacement control. All samples were tested at the displacement rate of 0.125 mm/s, which resulted in sample strain rates, calculated from video strain measurements, ranging from 9.1×10^{-4} s^{-1} to 1.9×10^{-3} s^{-1} depending on several factors including, but not always limited to mechanical compliance, sample slippage, and settling of the wedge action grips used.

[0067] The results of tensile testing of the sheet from the alloys processed to different thicknesses are listed in Table 7 representing Step 3 in FIG. **1**. For Alloy 1, tensile elongation is measured in the range from 44.9 to 51.1%, for Alloy 27 in the range from 63.8 to 73.8%, and for Alloy 37 in the range from 6.0 to 7.0%. Tensile elongation as a function of the sheet thickness is illustrated in FIG. **6** for the selected alloys. FIG. **8** and FIG. **9** show the yield strength and ultimate tensile strength of the sheet with different thicknesses for the selected alloys. The ultimate tensile strength is in a range from 1203 to 1269 MPa in Alloy 1 sheet, from 972 to 1067 MPa in Alloy 27 sheet, and from 1493 to 1614 MPa in Alloy 37 sheet. Yield strength varies from 375 to 444 MPa in Alloy 1 sheet, from 367 to 451 MPa in Alloy 27 sheet, and from 612 to 820 MPa in Alloy 37 sheet.

TABLE 7

Tensile Properties of the Sheet from Selected Alloys at Thickness < 1.2 mm

Alloy	Thickness (mm)	Tensile Elongation (%)	Ultimate Tensile Strength (MPa)	Yield Strength (MPa)
Alloy 1	0.52	49.2	1269	444
	0.52	51.1	1247	440
	0.52	48.1	1203	433
	0.76	49.8	1241	406
	0.76	50.7	1238	409
	0.77	44.9	1247	413
	0.99	46.8	1253	375
	1.01	45.4	1262	381
	1.01	46.7	1251	384

TABLE 7-continued

Tensile Properties of the Sheet from Selected Alloys at Thickness < 1.2 mm

Alloy	Thickness (mm)	Tensile Elongation (%)	Ultimate Tensile Strength (MPa)	Yield Strength (MPa)
	1.02	47.6	1255	396
	1.03	50.3	1237	384
	1.04	45.6	1246	396
Alloy 27	0.21	63.8	1067	440
	0.21	64.9	1063	445
	0.37	67.1	1039	429
	0.38	68.6	1040	427
	0.38	69.5	1022	425
	0.51	68.2	1060	451
	0.52	68.5	1056	449
	0.75	71.8	1019	413
	0.76	71.1	1012	412
	1.02	72.9	972	367
	1.03	73.8	1005	380
	1.04	71.7	1001	369
Alloy 37	0.30	6.4	1579	727
	0.32	6.0	1493	782
	0.32	6.5	1523	790
	0.50	6.6	1603	820
	0.51	6.3	1614	754
	0.51	6.0	1602	775
	0.75	6.7	1602	710
	0.77	6.6	1590	612
	0.99	6.9	1589	659
	1.01	6.8	1588	673
	1.01	6.9	1596	648

[0068] This Case Example demonstrates that tensile ductility of alloys herein is maintained even at sheet thickness as small as 0.2 mm demonstrating an average total elongation no less than that in the corresponding sheet with 1.2 mm thickness and above minus 7.3%. An average ultimate tensile strength is a range of ±35 MPa of that in the corresponding sheet with 1.2 mm thickness and above with the yield strength in a range of ±98 MPa.

Case Example #4 Microstructure in Sheet from Selected Alloys at Different Thicknesses

[0069] The hot band from Alloy 1, Alloy 2, Alloy 27, and Alloy 37 was cold rolled in to sheets with different thicknesses less than 1.2 mm through multiple cold rolling passes. Once the targeted gauge thickness was reached, samples were cut from each cold rolled sheet by wire EDM. The samples were annealed under conditions intended to simulate the thermal exposure expected during an industrial continuous annealing process. Samples were wrapped in stainless steel foil to prevent oxidation and loaded into a preheated furnace at 850° C. The microstructures of the cold rolled and annealed state were studied by SEM to show the structural change during processing. To prepare SEM samples, pieces were cut by EDM from the sheet and mounted in epoxy, and the sheet cross-sections were polished progressively with 9 μm, 6 μm and 1 μm diamond suspension solution, and finally with 0.02 μm silica. The SEM study was conducted using an EVO-60 scanning electron microscope manufactured by Carl Zeiss SMT Inc.

[0070] FIG. **10** shows microstructures in Alloy 1 sheet samples with different thicknesses. Cold rolled structure is shown in FIG. **10***a* and FIG. **10***c* in the center of the sheet with thickness of 0.7 and 0.5 mm, respectively. The cold rolled sample bears the highly deformed microstructure in which grain boundaries are difficult to see. The microstructure in these sheet samples after annealing is shown in FIG. **10***b* and FIG. **10***d* represented by the recrystallized structure with equiaxed grains and clear grain boundaries.

[0071] FIG. **11** shows microstructures in Alloy 2 sheet samples with different thicknesses. Cold rolled structure is shown in FIG. **11***a*, FIG. **11***c* and FIG. **11***e* in the center of the sheet with thickness of 1.0, 0.5 and 0.2 mm, respectively. The cold rolled sample bears the highly deformed microstructure in which grain boundaries are difficult to see. The microstructure in these sheet samples after annealing is shown in FIG. **11***b*, FIG. **11***d* and FIG. **11***f* represented by recrystallized structure with equiaxed grains and clear grain boundaries.

[0072] The structure in the sheet samples from Alloy 27 is similar to Alloy 1 and Alloy 2 and is shown in FIG. **12**. The recrystallized microstructure in the sheet from Alloy 27 has fewer twins as compared to other studied alloys, as shown in FIG. **12***b*, FIG. **12***d* and FIG. **12***f*.

[0073] Alloy 37 is a different type of the alloy in which the annealing does not lead to the typical recrystallized structure formation. FIG. **13** shows the structures at the center of the sheet from Alloy 37 with different thicknesses after cold rolling and after cold rolling and annealing. Only a small difference between the cold rolled and the annealed structures is observed. Corresponding samples at different thicknesses have effectively identical structures.

[0074] This Case Example demonstrates that microstructure is maintained in alloys herein after annealing of cold rolled sheet independently from the final sheet thickness.

Case Example #5: Strain Rate Effect on Tensile Ductility of the Sheet from Alloy 2

[0075] Slabs of Alloy 2 were cast according to the atomic compositions provided in Table 1. Following casting, the slabs were hot rolled through successively smaller roll gaps to produce hot band coils in the range of 2 to 5 mm thick, which were subsequently subjected to cold rolling and annealing cycles until the targeted thickness of approximately 1.4 mm was achieved representing sheet material in Step 2 in FIG. **2**. Annealing was done in this case in the temperature range from 950 to 1050° C.

[0076] The tensile properties of the material were characterized as a function of strain rate. Tensile samples were tested at 0.0007 s^{-1}, 0.7 s^{-1}, 10 s^{-1}, 100 s^{-1}, 500 s^{-1} and 1200 s^{-1} nominal strain rates in the ASTM D638 Type V tensile geometry shown in FIG. **14**. Tensile samples tested at strain rates from 0.0007 s^{-1} to 500 s^{-1} were tested on an MTS servo-hydraulic test frame. Samples were inserted into grips and load was applied by raising the crosshead at speeds necessary to produce the nominal strain rates. A slack adapter consisting of a cup and cone rod assembly was used at strain rates greater than 1 s^{-1} to allow the test frame to achieve the targeted constant strain rate prior to applying load to the specimen. An instrumented bar was used at 500 s^{-1} to mitigate the effects of standing waves in the test apparatus that occurred during high strain rate testing. At 1200 s^{-1} strain rate, a split Hopkinson bar (SHB) was used. The SHB device was composed of 25.4 mm diameter 7075 Al incident and transmission bars, with the test specimen tightly gripped between the Al bars. Strain gauges were used on the transmission and incident bars to measure strain in the bars. A striker tube was launched around the incident tube towards the striker plate to generate the tensile strain pulse and the strain within the sample was recorded. A schematic diagram of the SHB is provided in FIG. **15**.

[0077] Strain in the tensile samples was measured by a mechanical extensometer at 0.0007 s^{-1} and 0.7 s^{-1} strain rates. Digital Image Correlation (DIC) was used to measure strain for samples tested at 10 s^{-1}, 100 s^{-1}, and 500 s^{-1}. Five tensile samples were tested at all strain rates. In the case of one sample at 0.0007 s^{-1} strain rate, a malfunction occurred that resulted in the loss of the sample. Two samples tested at 1200 s^{-1} did not fail during testing.

[0078] Measured strain at failure is provided in Table 8. The measured strain is plotted as function of strain rate in FIG. **16**. Table 9 provides the average ductility as measured by tensile elongation at failure for each nominal strain rate. Note that the average tensile elongation measured at all strain rates is close to the overall average of 55.5% across all strain rates. At strain rates from 0.0007 s^{-1} to 500 s^{-1}, the average tensile elongation at failure is within approximately ±3% of the total average of all tests. Tests at 1200 s^{-1} were measured to possess higher tensile elongation at failure than all other tests, however due to the nature of this test methodology these values may be measured slightly higher than actual values. Ultimate tensile strength is measured in a range from 944 to 1187 MPa with yield strength from 347 to 512 MPa (Table 10).

[0079] Tensile properties in Tables 8 through 10 represents sheet material in Step 3 in FIG. **2**.

TABLE 8

Tensile Elongation of Alloy 2 Sheet Samples Tested at Different Strain Rates

Nominal Strain Rate (s^{-1})	Strain Measurement Technique	Measured Strain Rate (s^{-1})	Elongation at Failure (%)
0.0007	Extensometer	0.000803	62.4
0.0007	Extensometer	0.000768	44.6
0.0007	Extensometer	0.000713	44.9
0.0007	Extensometer	0.000749	59.2
0.7	Extensometer	0.644	57.1
0.7	Extensometer	0.682	53.7
0.7	Extensometer	0.632	54.4
0.7	Extensometer	0.634	54.5
0.7	Extensometer	0.650	52.5
10	DIC	5.83	49.5
10	DIC	6.03	50.4
10	DIC	6.07	54.6
10	DIC	6.02	49.5
10	DIC	5.78	54
100	DIC	65.7	55.7
100	DIC	87.9	52.7
100	DIC	88.5	56.2
100	DIC	86.2	54.5
100	DIC	85.4	57.1
500	DIC	438	57.0
500	DIC	442	57.3
500	DIC	440	56.2
500	DIC	414	57.5
500	DIC	425	56.1
1200	SHB	1169	64.9
1200	SHB	1222	67.7
1200	SHB	1152	63.1

TABLE 9

Average Tensile Elongation of Sheet from Alloy 2 at Each Strain Rate

Nominal Strain Rate (s^{-1})	Strain Measurement Technique	Elongation at Failure (%)
0.0007	Extensometer	52.8
0.7	Extensometer	54.4
10	DIC	52.0
100	DIC	55.2
500	DIC	56.8
1200	SHB	65.2
	Overall Average	56.0

TABLE 10

Strength Characteristics of Alloy 2 Sheet Tested at Different Strain Rates

Nominal Strain Rate (s^{-1})	Strain Measurement Technique	Measured Strain Rate (s^{-1})	Yield Strength (MPa)	Ultimate Tensile Strength (MPa)
0.0007	Extensometer	0.000803	375	1159
0.0007	Extensometer	0.000768	356	1151
0.0007	Extensometer	0.000713	365	1171
0.0007	Extensometer	0.000749	371	1187
0.7	Extensometer	0.644	354	1014
0.7	Extensometer	0.682	454	992
0.7	Extensometer	0.632	431	1017
0.7	Extensometer	0.634	416	1024
0.7	Extensometer	0.650	442	1006
10	DIC	5.83	455	989
10	DIC	6.03	422	979
10	DIC	6.07	424	980
10	DIC	6.02	450	975
10	DIC	5.78	347	977
100	DIC	65.7	483	956
100	DIC	87.9	499	944
100	DIC	88.5	488	953
100	DIC	86.2	505	956
100	DIC	85.4	459	948
500	DIC	438	425	1020
500	DIC	442	409	1030
500	DIC	440	500	1010
500	DIC	414	444	1030
500	DIC	425	512	1020
1200	SHB	1169	—	946
1200	SHB	1222	—	965
1200	SHB	1152	—	972

[0080] This Case Example demonstrates that tensile ductility of alloys herein is retained across a relatively large range of strain rates of 0.007 to 1200 s^{-1}. A measured average ultimate tensile strength is 62 MPa lower at higher strain rates and average yield strength is 59 MPa lower.

Case Example #6 Strain Rate Effect on Microstructure in the Sheet from Alloy 2

[0081] The microstructures of the samples from sheet from Alloy 2 tested at five different strain rates ranging from 0.0007 s^{-1} to 1200 s^{-1} (see Case Example #5) were studied by TEM. For TEM study, pieces are cut from the gauge section of deformed samples by diamond saw. Grinding and polishing are then undertaken to make thin foils from the cut pieces. The polishing was conducted progressively with 9 μm, 6 μm and 1 μm diamond suspension solution, and finally with 0.02 μm silica. Foils with thickness of 70 to 80 μm were obtained after the polishing. Discs of 3 mm in diameter were punched from the foils and the final polishing was fulfilled with electropolishing using a twin-jet polisher. The chemical solution used was a 30% Nitric acid mixed in Methanol base. In case of insufficient thin area for TEM observation, the TEM specimens may be ion-milled using a Gatan Precision Ion Polishing System (PIPS). The ion-milling usually is done at 4.5 keV, and the inclination angle is reduced from 4° to 2° to open up the thin area. The TEM studies were done using a JEOL 2100 high-resolution microscope operated at 200 kV.

[0082] FIG. **17** shows the bright-field TEM images of the sample tested at 1200 s^{-1}. It can be seen that deformation twins are prominent in the high rate deformed sample which are a forming of twinning which does not occur through mechanical deformation but during heat treatment. The twins are distinct and sharp, suggesting that they are newly formed from the deformation. With twinning being a deformation mode in the sample, phase transformation is reduced since the deformation twins maintain austenitic structure. Twinning as a method of deformation can be seen in the sample deformed at strain rates of 500, 100, 10, and 0.7 s^{-1}, as shown in FIG. **18** through FIG. **21**. The sample deformed at strain rate of 0.0007 s^{-1} has different structure as can be seen in FIG. **22** demonstrating a domination of dislocation with phase transformation during deformation that is evident from the Feritscope measurements in the sample gauges after deformation. As shown in FIG. **23**, the magnetic phases volume percent, which correlates to the transformed product phases, is highest in the case of deformation at low strain rate of 0.0007 s^{-1}.

[0083] This Case Example demonstrates the alteration of deformation mechanisms during deformation of the alloys herein with higher occurrence of twinning with increasing strain rate. Deformation by twinning at high strain rates suppresses the phase transformation (i.e. means that the total amount of ferrite produced is reduced) allowing to the retention of relatively high tensile ductility of the sheet material in a wide range of strain rates.

Case Example #7 Notch Effect on Tensile Properties of Sheet from Alloy 2

[0084] Slabs of Alloy 2 were cast according to the atomic compositions provided in Table 1. Following casting, the slabs were hot rolled through successively smaller roll gaps to produce hot band coils, which were subsequently subjected to cold rolling and annealing cycles until the targeted thickness of approximately 1.4 mm was achieved representing sheet in Step 2 in FIG. **3**.

[0085] Tensile specimens were cut from the sheet via wire EDM. The specimens had two notches, symmetric at about the center of the width and the length as showed in FIG. **24**. Samples were tested in tension with one grip fixed and the other moving at a fixed rate of 0.125 mm/s displacement rate. Tensile properties were measured on an Instron mechanical testing frame, utilizing Instron's Bluehill control and analysis software. All tests were run at ambient temperature in displacement control. A 50 mm gauge length was used centered on the notch. Stresses were calculated based on the nominal width not the notched width (FIG. **24**).

[0086] Tensile properties of the Alloy 2 sheet samples as a function of notch diameter and notch depth are listed in Table 11. Tensile elongation of notched samples ranged from 12.4% to 40.7%, yield strength ranged from 298 to 420 MPa, and ultimate tensile strength ranged from 636 to 1123 MPa. Effect of notch diameter with constant depth of 0.5 mm on tensile properties of the sheet from Alloy 2 is illustrated in FIG. **25**. Changes in tensile properties of the sheet with half circle notches as a function of notch diameter are shown in FIG. **26**. This data represents sheet in Step 3 in FIG. **3**.

TABLE 11

Tensile Properties of Notched Specimens from Alloy 2 Sheet

Notch Diameter (mm)	Notch Depth (mm)	Strain at Break (%)	Ultimate Tensile Strength (MPa)	Yield Strength (MPa)
0.35	0.175	22.1	913	407
0.35	0.175	26.6	991	409
0.35	0.175	21.2	909	420
0.5	0.25	17.7	844	416
0.5	0.25	18.9	874	411
0.5	0.25	22.0	923	397
1	0.5	14.4	789	406
1	0.5	17.3	827	386
1	0.5	18.2	862	408
2	1	16.7	802	386
2	1	17.9	839	375
2	1	23.0	875	345
4	2	15.6	764	371
4	2	18.7	816	372
4	2	17.9	811	377
6	3	12.4	636	314
6	3	13.1	646	308
6	3	12.9	651	298
2	0.5	22.8	926	405
2	0.5	26.3	992	405
2	0.5	25.8	992	397
4	0.5	27.4	982	394
4	0.5	32.8	1054	391
4	0.5	31.7	1056	396
6	0.5	34.8	1071	383
6	0.5	40.7	1123	384

[0087] This Case Example demonstrates an increase in tensile elongation of the notched samples from alloys herein with increasing notch diameter at constant depth. In the case of increasing depth, average elongation is shown to be independent of the notch depth (half circle).

Case Example #8 Ductile Fracture Surface in Notched Sample after Testing

[0088] SEM fracture analysis was performed on selected notched specimens from Alloy 2 sheet after tensile testing (see Case Example #7). Two samples with notch radius of 1.0 and 6.0 mm were selected for examination (Table 12). The SEM study was conducted using an EVO-60 scanning electron microscope manufactured by Carl Zeiss SMT Inc.

TABLE 12

Samples for SEM Analysis

Samples	Notch Diameter (mm)	Notch Depth (mm)
1	1.0	0.5
2	6.0	0.5

[0089] In FIG. **27** and FIG. **28**, SEM images of fracture surface after tensile testing are shown for Sample 1 and Sample 2, respectively. Images are taken from the center of the fracture cross section and close to the edge. Both samples demonstrated ductile fracture. There is no difference in fracture mode between the center and the edge of the fracture cross section although finer structure is found closer to the edge.

[0090] This Case Example demonstrates that notch introduction into the sheet material from alloys herein does not cause brittle catastrophic failure. Notched samples after testing have demonstrated ductile fracture.

[0091] The alloys herein may be utilized in variety of applications. For example, the alloys herein may be positioned in vehicular frame, vehicle chassis or vehicle panel. In addition, the alloys herein may be utilized for a storage tank, freight car, or railway tank car. Railway tank cars may specifically include tanks, jacketed tanks or tanks with a headshield. Other applications include body armor, metallic shield, military vehicles, and armored vehicle Such applications apply to the alloys produced according to any one of FIG. **1**, FIG. **2** and/or FIG. **3**.

1. A method to retain mechanical properties in a metallic sheet alloy at reduced thickness comprising:

a. supplying a metal alloy comprising at least 70 atomic % iron and at least four or more elements selected from Si, Mn, Cr, Ni, Cu, or C, melting said alloy, cooling at a rate of <250 K/s, and solidifying to a thickness of 25.0 mm up to 500 mm;

b. processing said alloy into sheet form with thickness T_1 with the sheet having a total elongation of X_1 (%), an ultimate tensile strength of Y_1 (MPa), and a yield strength of Z_1 (MPa);

c. further processing said alloy into a second sheet with reduction in thickness $T_2<T_1$ with the second sheet having a total elongation of $X_2=X_1\pm10\%$, an ultimate tensile strength of $Y_2=Y_1\pm50$ MPa, and a yield strength of $Z_2=Z_1\pm100$ MPa.

2. The method of claim **1** wherein said at least 70 atomic percent iron is combined with five or more elements that are selected from Si, Mn, Cr, Ni, Cu, or C.

3. The method of claim **1** wherein said at least 70 atomic percent iron is combined with all six elements: Si, Mn, Cr, Ni, Cu, and C.

4. The method of claim **1** wherein the levels of the four elements that are selected are as follows: Si (1.14 to 6.13 atomic percent), Mn (3.19 to 15.17 atomic percent), Cr (0.78 to 8.64 atomic percent); Ni (0.9 to 11.44 atomic percent), Cu (0.37 to 1.87 atomic percent).

5. The method of claim **1** wherein said alloy formed in step (b), exhibits X_1 (12% to 80%), Y_1 (700 MPa to 2100 MPa), and Z_1 (250 MPa to 1500 MPa).

6. The method of claim **1** wherein said alloy formed in step (b), exhibits a thickness from 1.2 mm to 10.0 mm.

7. The method of claim **1** wherein said alloy formed in step (c), exhibits X_2 (2 to 90%), Y_2 (650 MPa to 2150 MPa), and Z_2 (150 MPa to 1600 MPa).

8. The method of claim **1** wherein said alloy formed in step (c), exhibits a thickness from 0.2 mm to <1.2 mm.

9. The method of claim **1** wherein said alloy formed in step (c) is positioned in a vehicular frame, vehicular chassis, or vehicular panel.

10. The method of claim **1** wherein said alloy formed in step (c) is positioned in a storage tank, freight car, or railway tank car.

11. A method to retain mechanical properties in a metallic sheet alloy at relatively high strain rates comprising:

a. supplying a metal alloy comprising at least 70 atomic % iron and at least four or more elements selected from

Si, Mn, Cr, Ni, Cu, or C and melting said alloy and cooling at a rate of <250 K/s and solidifying to a thickness of 25.0 mm up to 500 mm;

b. processing said alloy into sheet form with thickness from 1.2 mm to 10.0 mm with the sheet having a total elongation of X_1 (%), an ultimate tensile strength of Y_1 (MPa), and a yield strength of Z_1 (MPa) when tested at a strain rate S_1;

c. deforming the sheet from said alloy at a strain rate $S_2>S_1$ with the sheet having a total elongation of $X_3=X_1\pm7\%$, ultimate tensile strength $Y_3=Y_1\pm200$ MPa, and yield strength $Z_3=Z_1\pm50$ MPa.

12. The method of claim **11** wherein said at least 70 atomic percent iron is combined with five or more elements that are selected from Si, Mn, Cr, Ni, Cu, or C.

13. The method of claim **11** wherein said at least 70 atomic percent iron is combined with all six elements: Si, Mn, Cr, Ni, Cu, and C.

14. The method of claim **11** wherein the levels of the four elements that are selected are as follows: Si (1.14 to 6.13 atomic percent), Mn (3.19 to 15.17 atomic percent), Cr (0.78 to 8.64 atomic percent); Ni (0.9 to 11.44 atomic percent), Cu (0.37 to 1.87 atomic percent).

15. The method of claim **11** wherein said alloy formed in step (b), exhibits X_1 (12% to 80%), Y_1 (700 MPa to 2100 MPa), and Z_1 (250 MPa to 1500 MPa).

16. The method of claim **11** wherein the strain rate S_1 is 0.007 s^{-1} to 0.0001 s^{-1}.

17. The method of claim **11** wherein said alloy formed in step (c), exhibits X_3 (5% to 87%), Y_3 (500 MPa to 2300 MPa), and Z_3 (200 MPa to 1550 MPa).

18. The method of claim **11** wherein the strain rate S_2 is >0.007 s^{-1} to 1200 s^{-1}.

19. The method of claim **11** wherein said processing in step (c) comprises roll forming, metal stamping or hydroforming.

20. The method of claim **11** wherein said alloy formed in step (c) is positioned in a vehicular frame, vehicular chassis, or vehicular panel.

21. The method of claim **11** wherein said alloy formed in step (c) is positioned in a storage tank, freight car, or railway tank car.

22. The method of claim **11** wherein said alloy formed in step (c) is positioned in body armor, shield, military vehicle, or armored vehicle.

23. A method to retain mechanical properties in a metallic sheet alloy comprising:

a. supplying a metal alloy comprising at least 70 atomic % iron and at least four or more elements selected from Si, Mn, Cr, Ni, Cu, or C and melting said alloy and cooling at a rate of <250 K/s and solidifying to a thickness of 25.0 mm up to 500 mm;

b. processing said alloy into sheet form with thickness from 1.2 mm to 10.0 mm with the sheet having a total elongation of X_1 (%), an ultimate tensile strength of Y_1 (MPa), and a yield strength of Z_1 (MPa);

c. introducing stress concentration sites and then deforming the sheet from said alloy with the sheet having a total elongation of $X_4\geq0.2X_1$ (%), an ultimate tensile strength $Y_4\geq0.5Y_1$ (MPa), and a yield strength $Z_4\geq0.6Z_1$ (MPa).

24. The method of claim **23** wherein said at least 70 atomic percent iron is combined with five or more elements that are selected from Si, Mn, Cr, Ni, Cu, or C.

25. The method of claim **23** wherein said at least 70 atomic percent iron is combined with all six elements: Si, Mn, Cr, Ni, Cu, and C.

26. The method of claim **23** wherein the levels of the four elements that are selected are as follows: Si (1.14 to 6.13 atomic percent), Mn (3.19 to 15.17 atomic percent), Cr (0.78 to 8.64 atomic percent); Ni (0.9 to 11.44 atomic percent), Cu (0.37 to 1.87 atomic percent).

27. The method of claim **23** wherein said alloy formed in step (b), exhibits X_1 (12% to 80%), Y_1 (700 MPa to 2100 MPa), and Z_1 (250 MPa to 1500 MPa).

28. The method of claim **23** wherein said processing in step (c) comprises roll forming, metal stamping or hydroforming.

29. The method of claim **23** wherein said alloy formed in step (c) is positioned in a vehicular frame, vehicular chassis, or vehicular panel.

30. The method of claim **23** wherein said alloy formed in step (c) is positioned in a storage tank, freight car, or railway tank car.

31. The method of claim **23** wherein said alloy formed in step (c) is positioned in body armor, shield, military vehicle, or armored vehicle.

* * * * *